Member of the Helmholtz Association

TEC
TRILATERAL
EUREGIO CLUSTER

JÜLICH
FORSCHUNGSZENTRUM

Radiation induced degradation of tungsten under thermal and plasma exposure and development of advanced tungsten materials

M. Berger[a], L. Buzi[a], J. Coenen[a], H. Greuner[b], A. Huber[a], A. Kreter[a], N. Lemahieu[a], B. Jaspers[a], J. Linke[a], A. Litnovsky[a], H. Maier[b], D. Matveev[a], G. Pintsuk[a], M. Rasinski[a], M. Reinhart[a], G. Sergienko[a], I. Steudel[a], T. Wegener[a], B. Unterberg[a], M. Wirtz[a],

[a]Forschungszentrum Jülich GmbH, Institute of Energy and Climate Research, 52425 Jülich, Germany

[b]Max-Planck-Institut für Plasmaphysik, Garching, Germany

2nd RCM on PWI with irradiated Tungsten and Tungsten Alloys in Fusion Devices,
08 - 11 September 2015, Seoul, Rep. of Korea

Outline of FZJ contributions

- Thermal shock behavior of irradiated and un-irradiated W grades
- Change of W micro- structure under simultaneous heat and particle loads and impact on W erosion and fuel retention in W
- Development of advanced tungsten materials with improved micro-structure
- Characterization of commercially available tungsten grades

A

Environmental conditions - test facilities

Environmental conditions

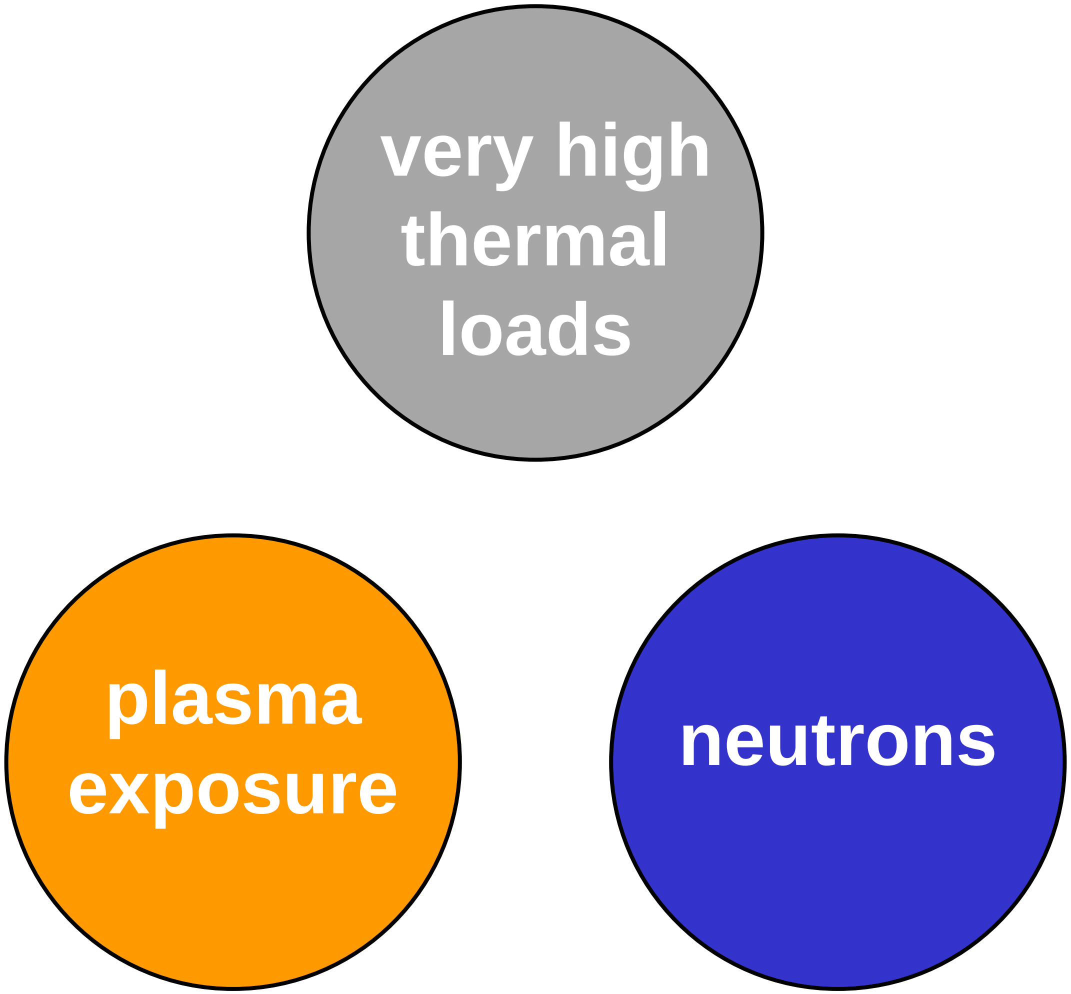

Environmental conditions

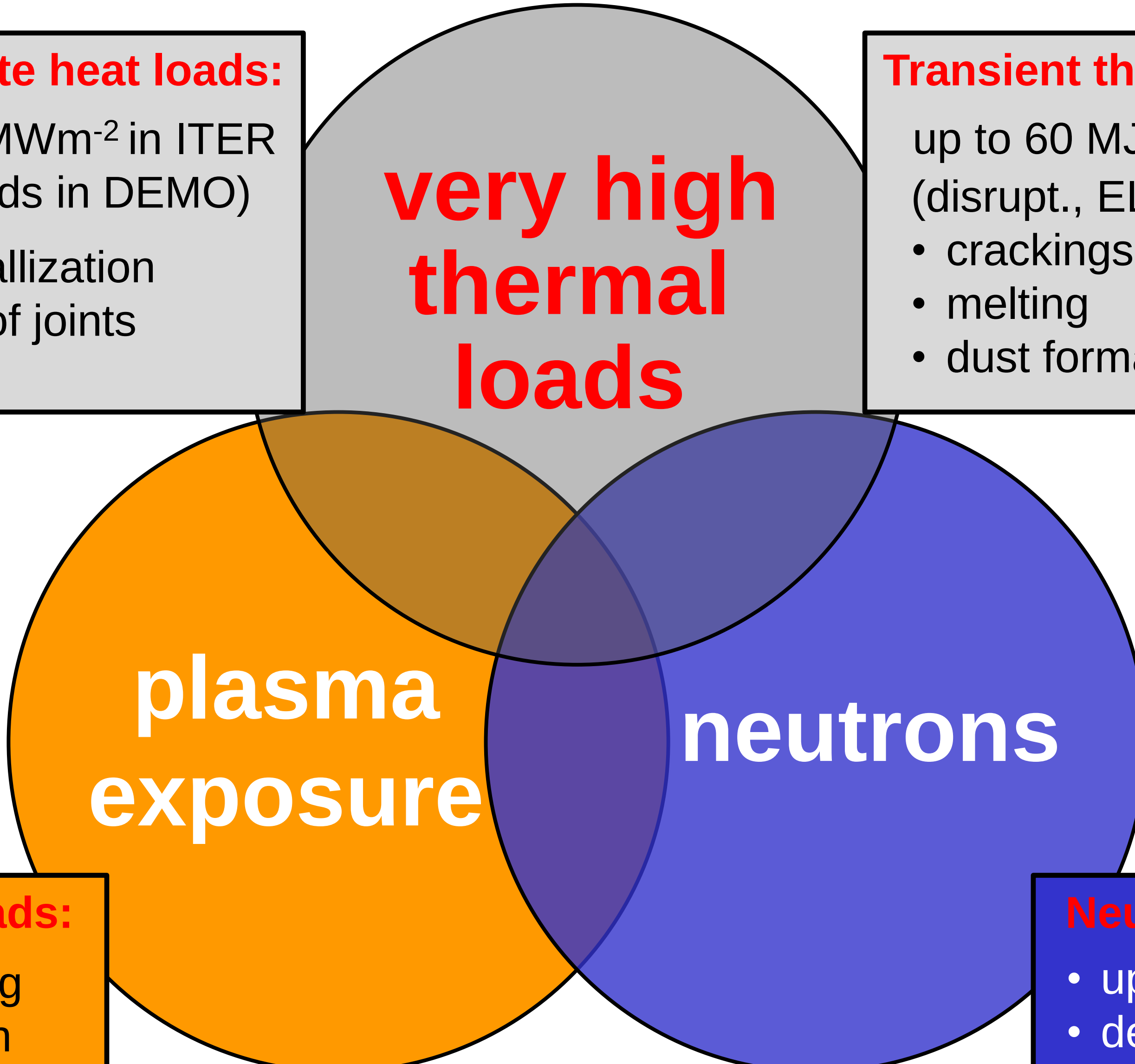

Steady state heat loads:

up to 20 MWm^{-2} in ITER
(lower loads in DEMO)

- recrystallization
- failure of joints

Transient thermal loads:

up to 60 MJm^{-2}
(disrupt., ELMs, VDEs)

- crackings
- melting
- dust formation

Plasma loads:

- sputtering
- hydrogen
- helium

Neutrons:

- up to 14 MeV
- defects
- transmutation

Facilities at FZJ

Electron beam facility JUDITH 1

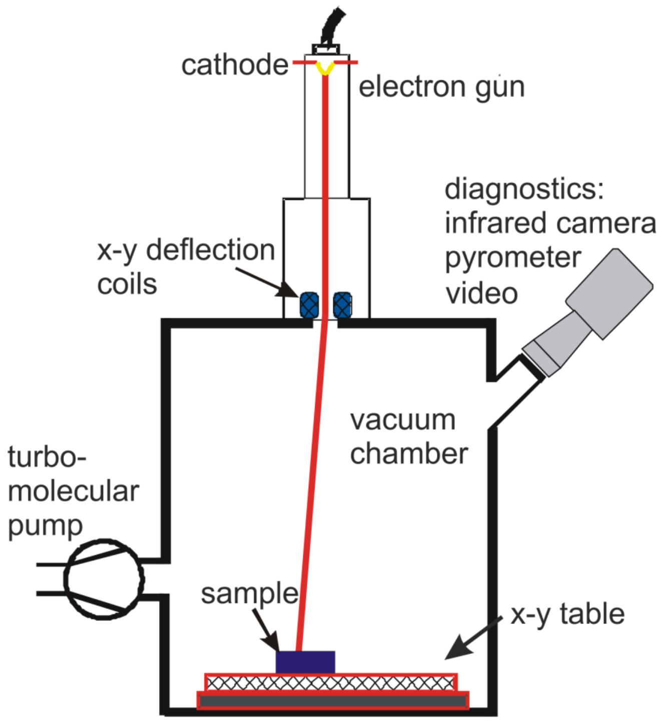

- max. power 60 kW
- acceleration voltage < 150 kV
- EB diameter ~1 mm (FWHM)

Linear plasma device PSI-2

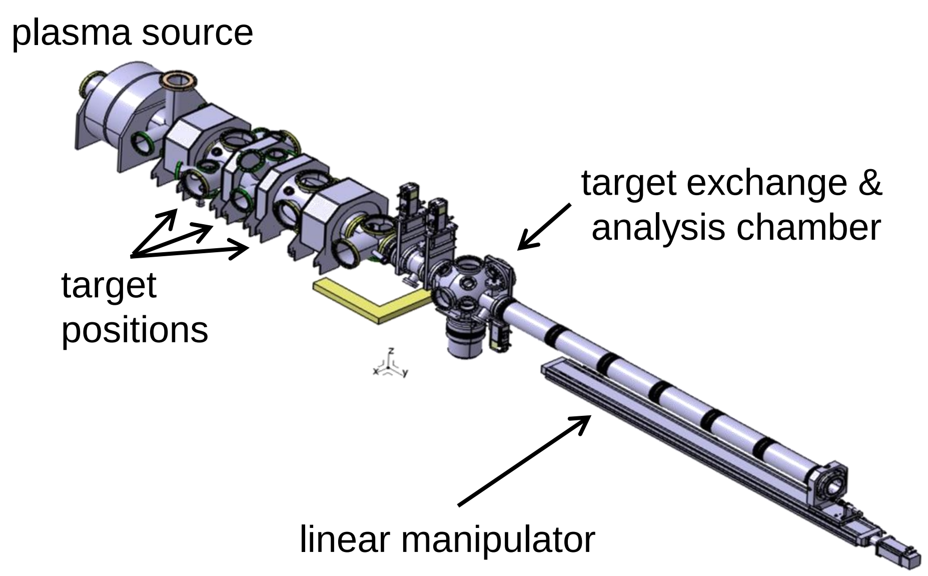

- plasma diameter 60 mm
- particle flux ≤ 10^{23} $m^{-2}s^{-1}$
- incident ion energy (bias) 10 – 300 eV
- Nd:YAG laser 1064 nm
- laser energy 32 J

B

Combined steady state and transient heat loads

Introduction

Expected heat loads in ITER divertor:

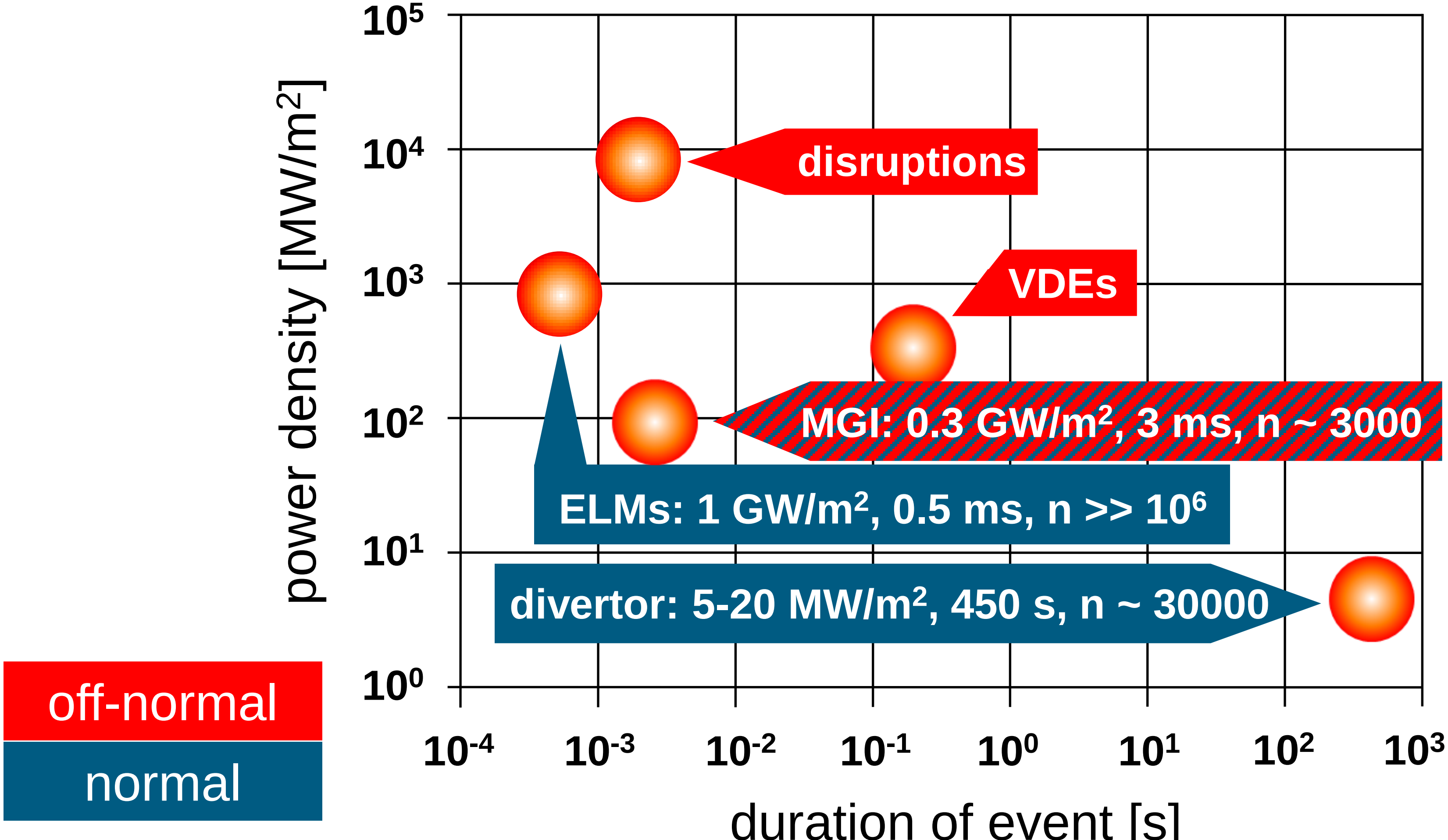

R. A. Pitts, et al., Journal of Nuclear Materials 438 (2013) S48-S56
J. Linke, Transactions of fusion science and technology 49 (2006) 455-464
A. Loarte et al., Plasma Physics and Controlled Fusion 45 (2003) 1549-1569

Experimental status

Successive (sequential) SSL + TL

- PILOT-PSI (H plasma) + JUDITH 2 (transient heat load)
- PSI-2 (H plasma + laser)

Simultaneous SSL + TL

- JUDITH 2 (heat load)
- PSI-2 (H plasma + laser)
- MAGNUM-PSI (H plasma)
- PILOT-PSI (H plasma)

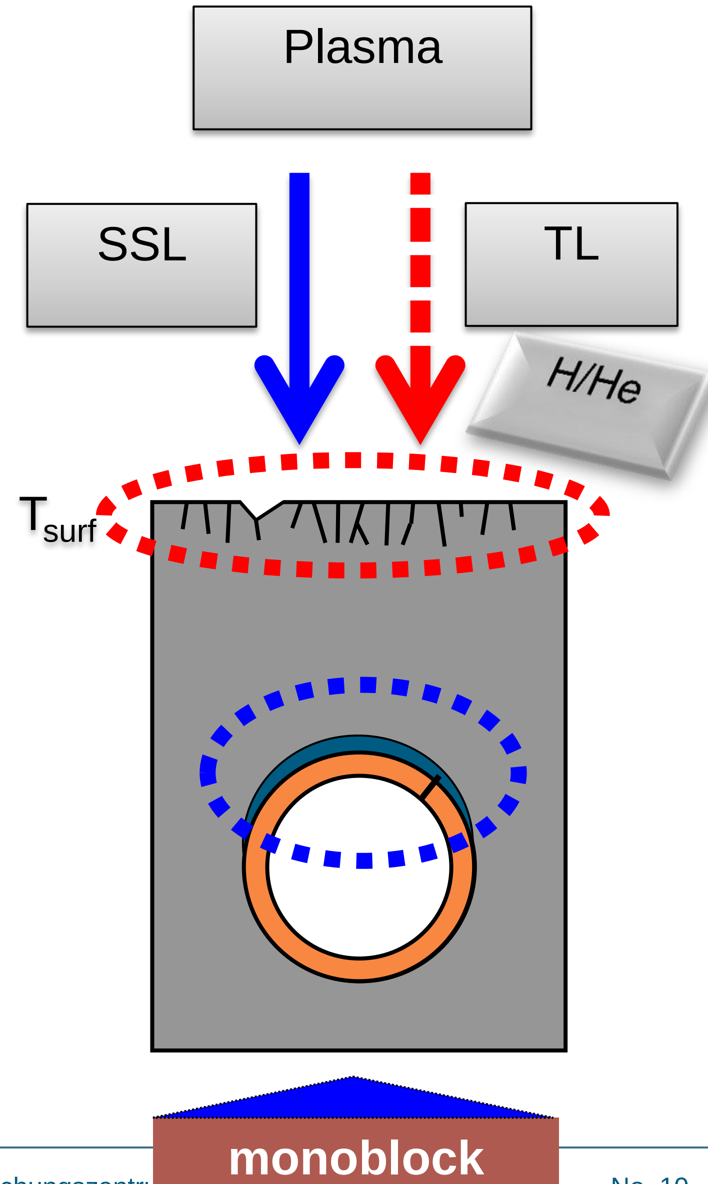

SSL = Steady state load
TL = Transient load

Experimental status

Simultaneous SSL + TL – JUDITH 2

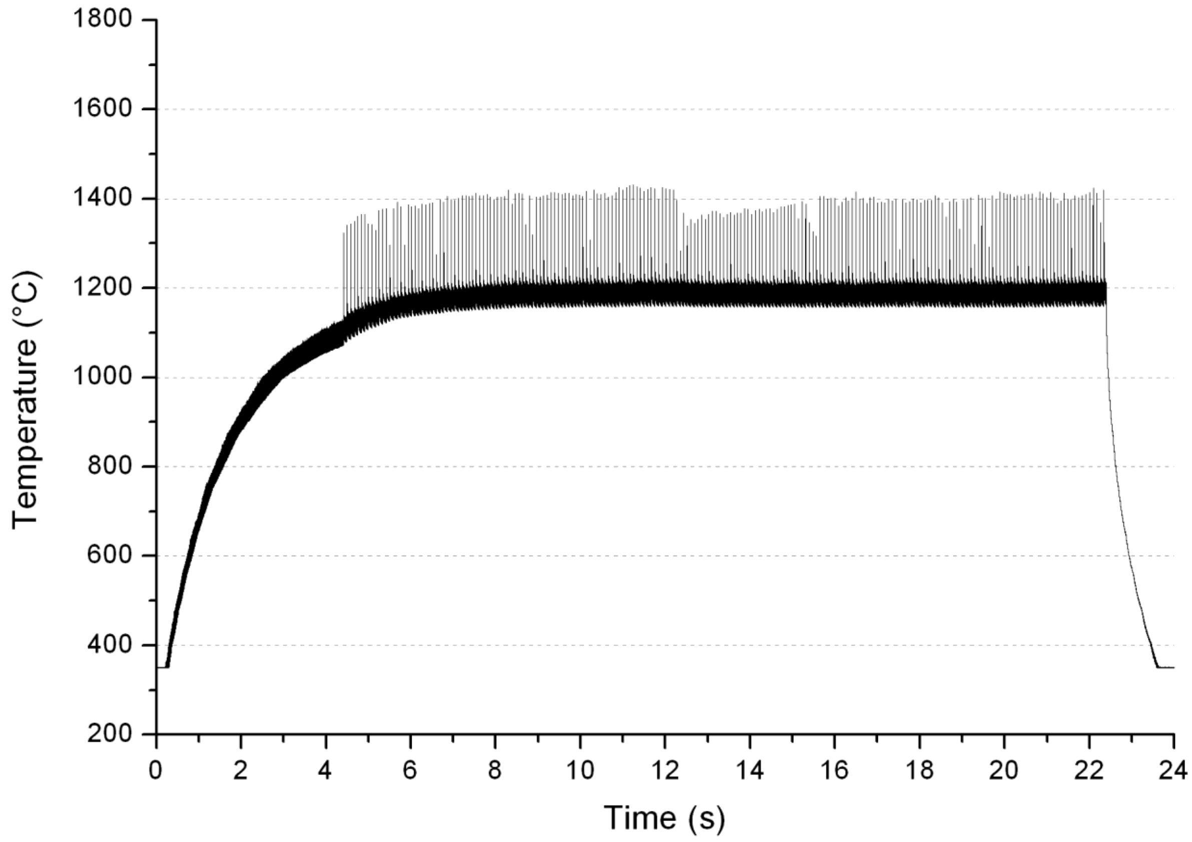

Experimental status

Simultaneous SSL + TL – JUDITH 2

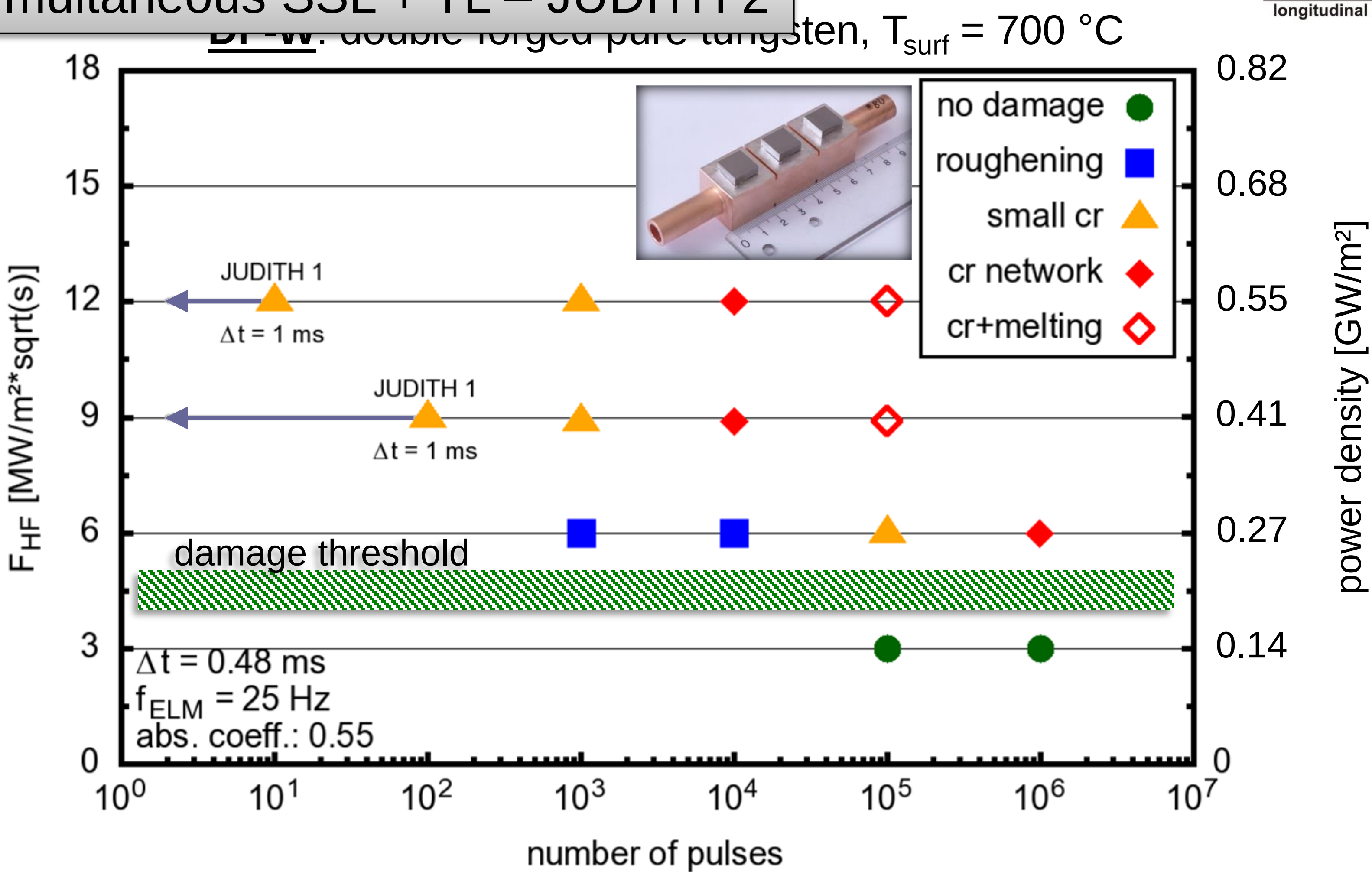

Th. Loewenhoff et al., Physica Scripta T145 (2011) 014057

Experimental status

Simultaneous SSL + TL – JUDITH 2

DF-W: double forged pure tungsten, T_{surf} = 700 °C

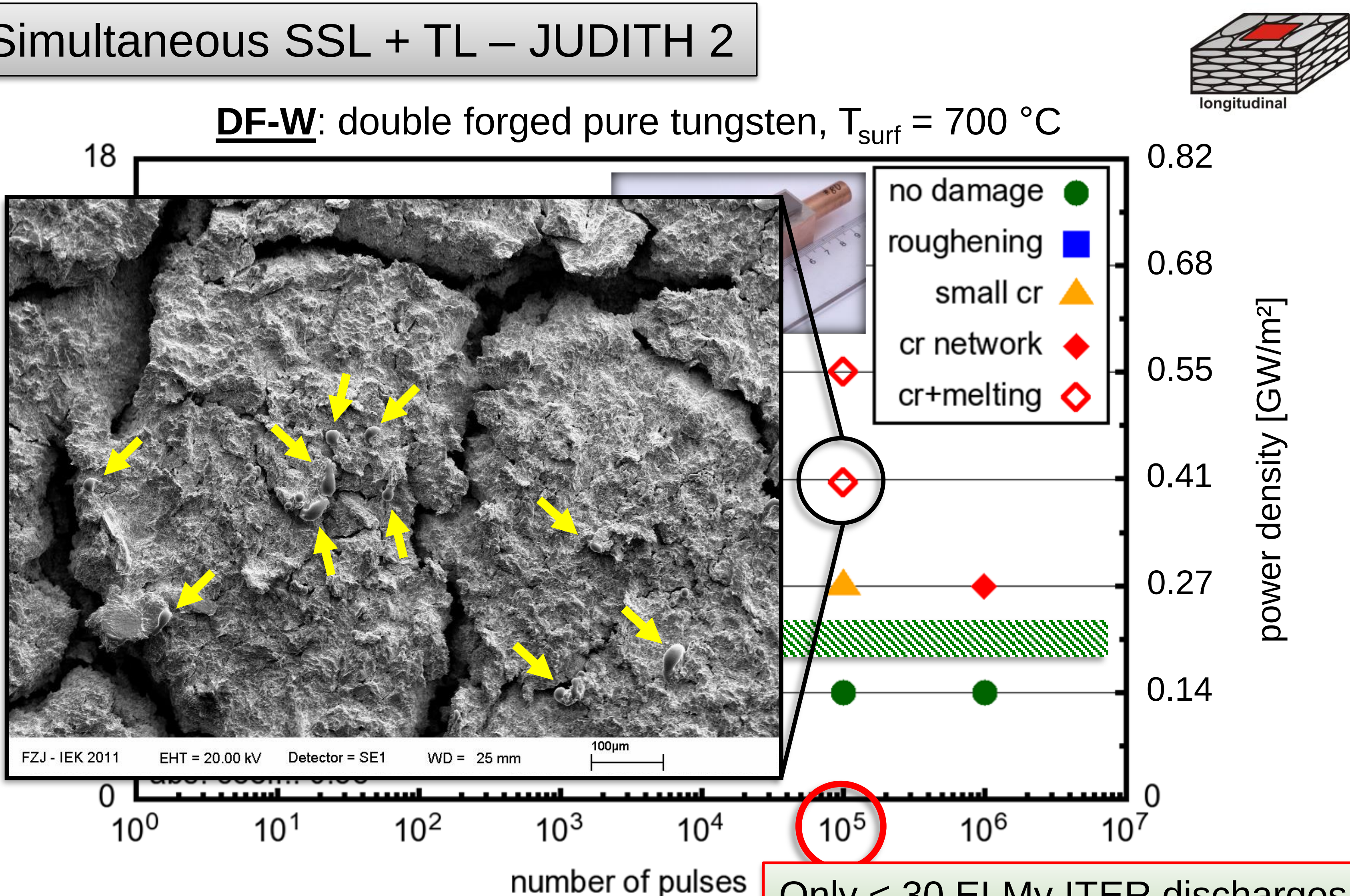

Only < 30 ELMy ITER discharges!

Th. Loewenhoff et al., Physica Scripta T145 (2011) 014057

Experimental status

Simultaneous SSL + TL – JUDITH 2

DF-W: double forged pure tungsten, T_{surf} = 700 °C

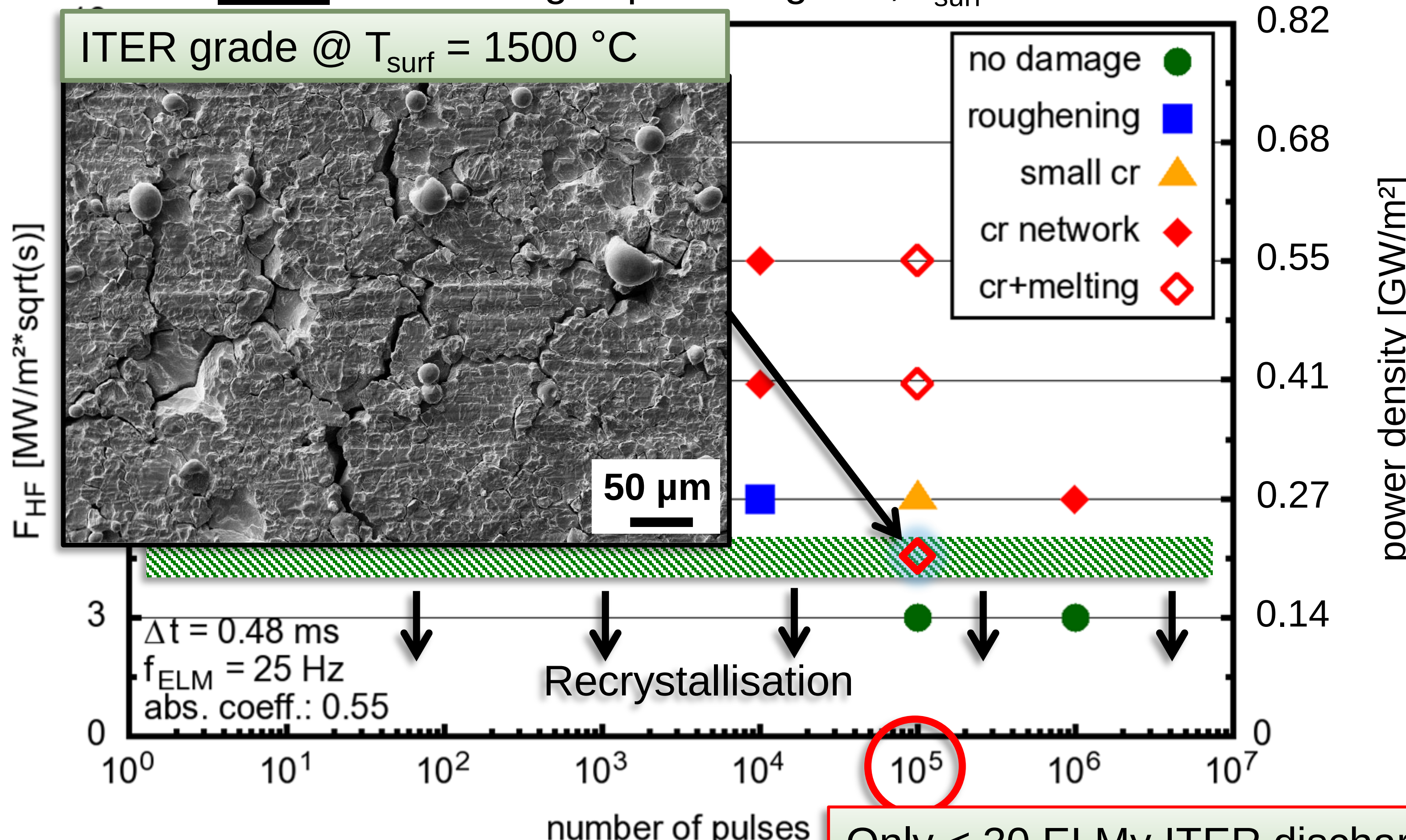

Only < 30 ELMy ITER discharges!

C

Combined particle and heat flux exposure of tungsten

Combined tests in PSI-2

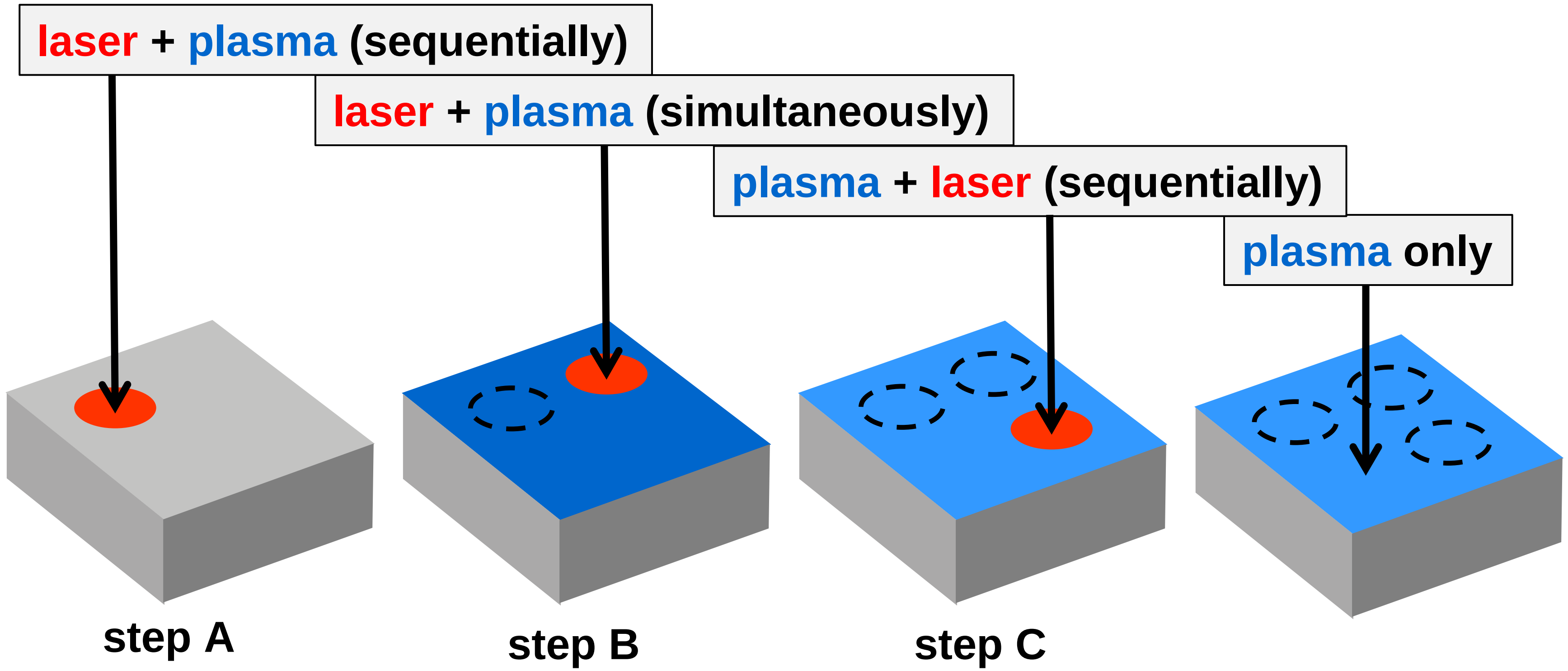

A laser beam exposure: Δt = 1 ms, n = 100 (1000)

B plasma exposure (H or He) of the full sample surface
+ simultaneous
laser beam exposure: Δt = 1 ms, n = 100 (1000)

C laser beam exposure: Δt = 1 ms, n = 100 (1000)

Thermal shock and H-loading in PSI-2

Laser beam
1000 ELM-like events at RT
absorbed power density: 0.3 GW/m²
pulse duration: 1 ms (f = 0.5 Hz)

H-Plasma

biasing voltage: - 60 V
source current: 150 A
plasma flux: 2.5 – 4.0 × 10^{21} $m^{-2}s^{-1}$

Laser ⇒ H-Plasma | **Simultaneous (ΔT ≈ 100 °C)** | **H-Plasma ⇒ Laser**

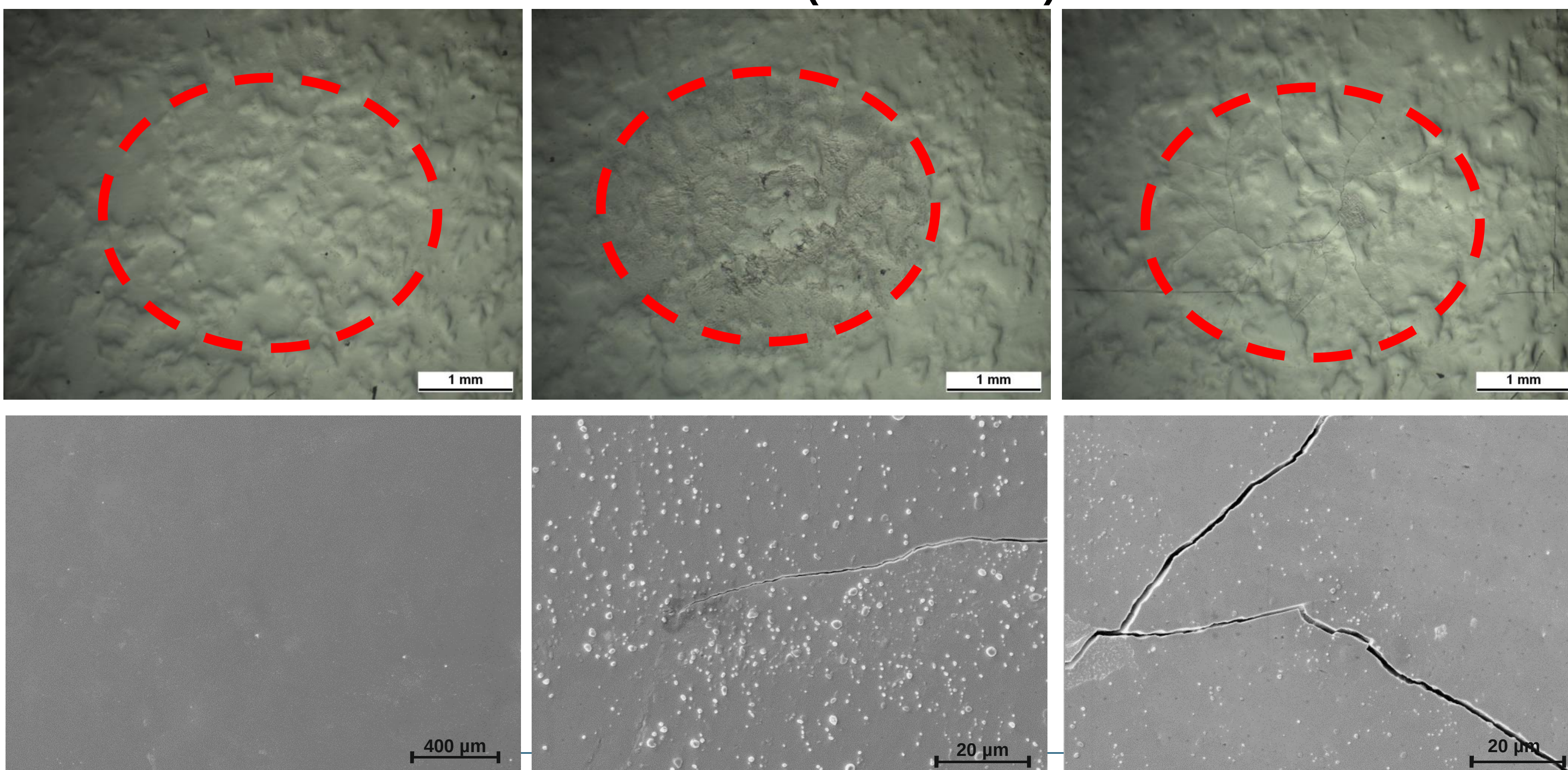

Thermal shock and H-loading in PSI-2

Laser beam

1000 ELM-like events at **400 °C**

absorbed power density: 0.38 GW/m^2

pulse duration: 1 ms (f = 0.5 Hz)

H-Plasma

biasing voltage: - 60 V

source current: 150 A

plasma flux: 2.5 – 4.0 × 10^{21} $m^{-2}s^{-1}$

Laser ⇒ H-Plasma | **Simultaneous** | **H-Plasma ⇒ Laser**

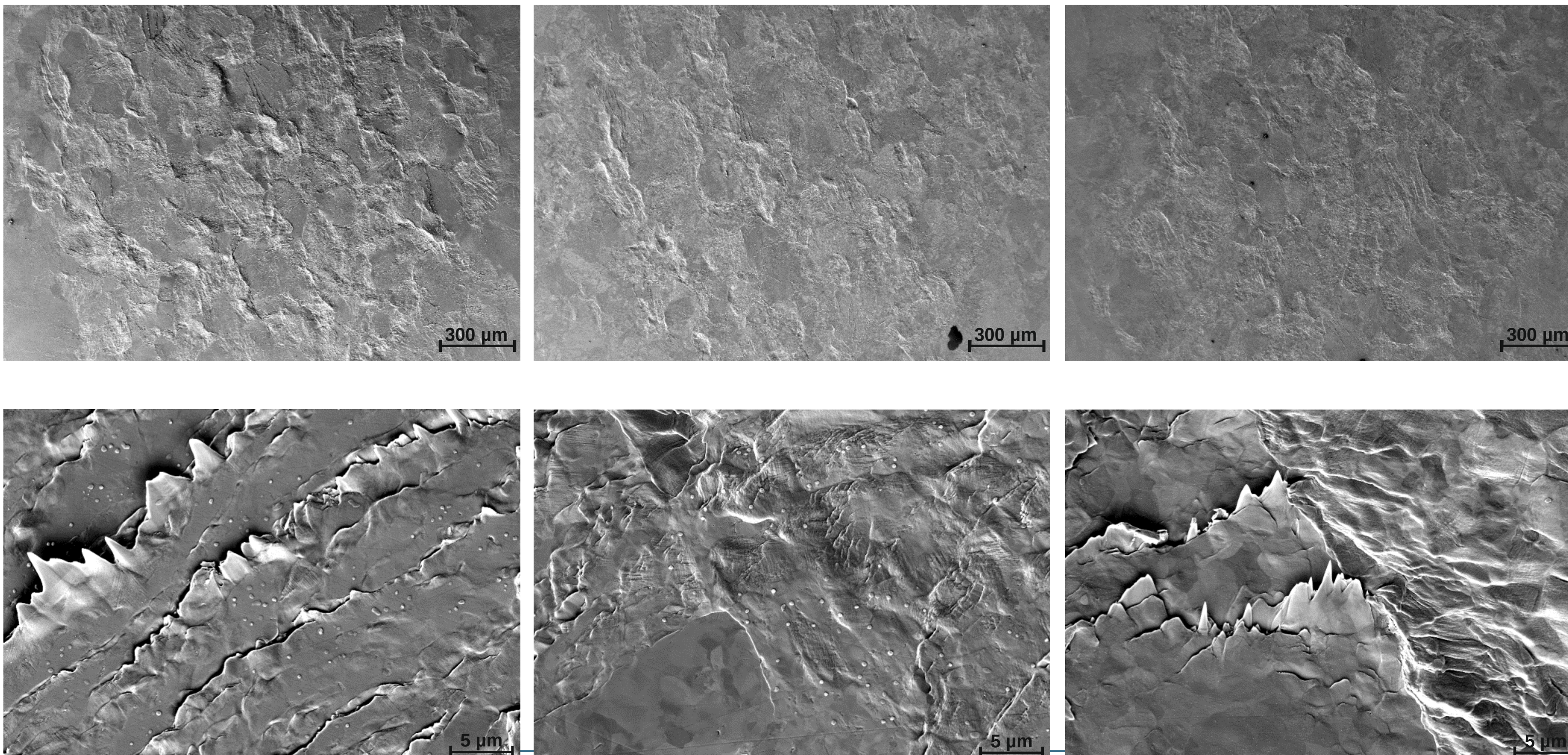

Surface structure analysis via FIB

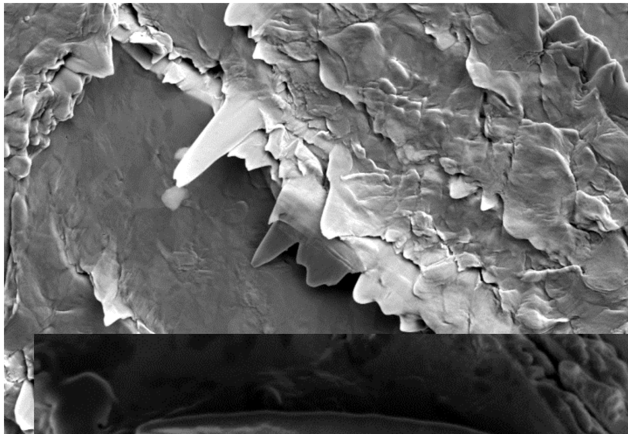

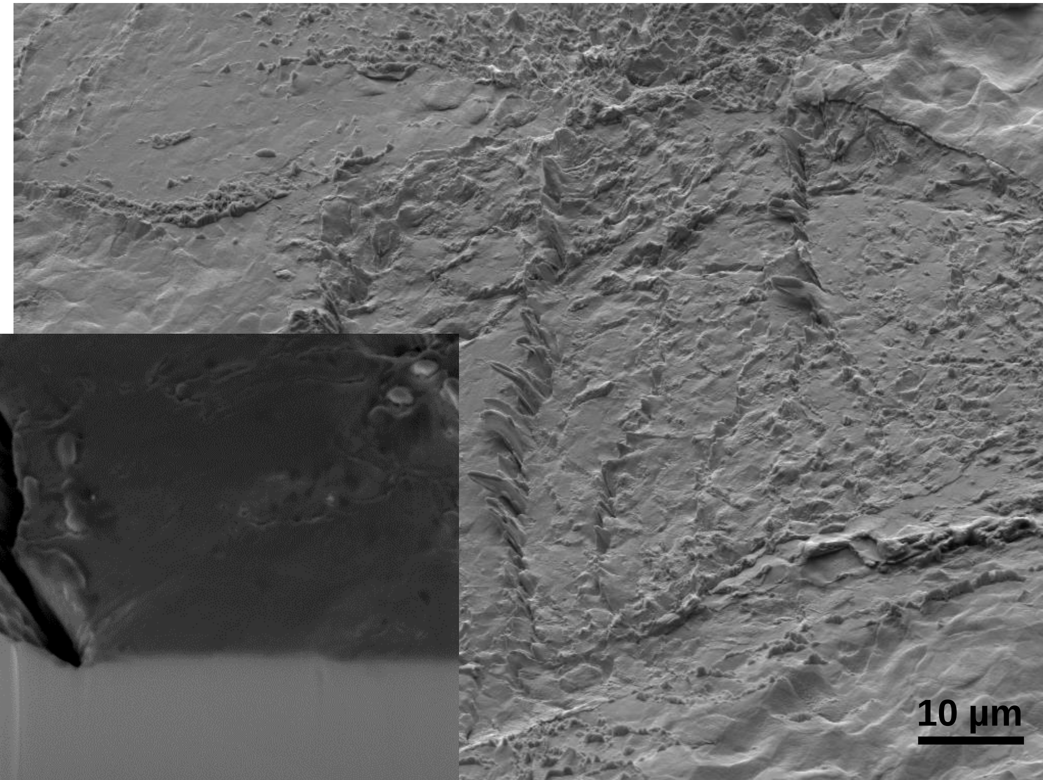

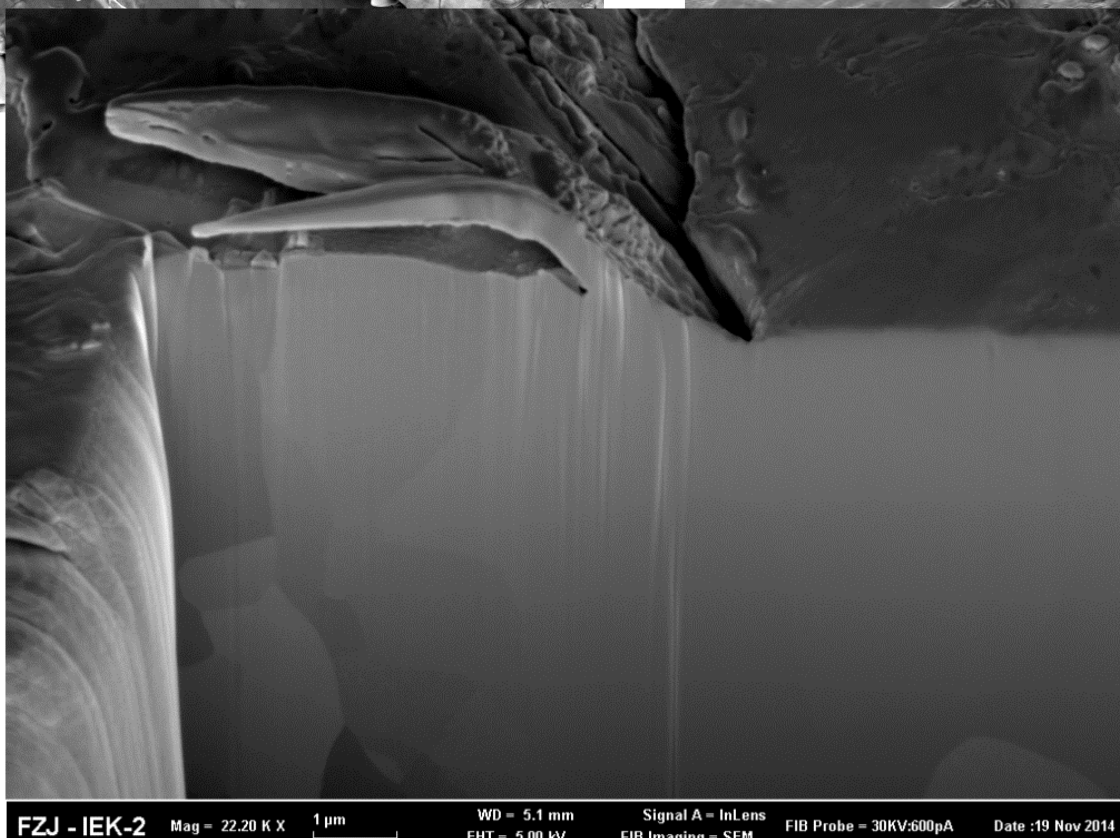

formation of melt droplets
erosion of scales

Thermal shock and H-loading in PSI-2

sequential tests

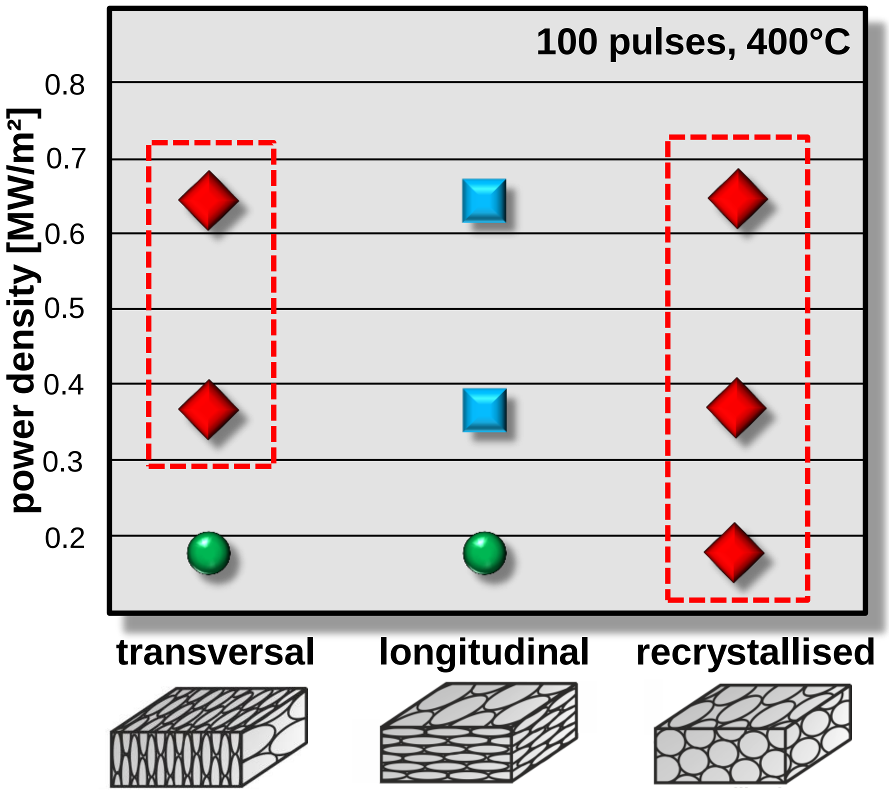

only laser tests

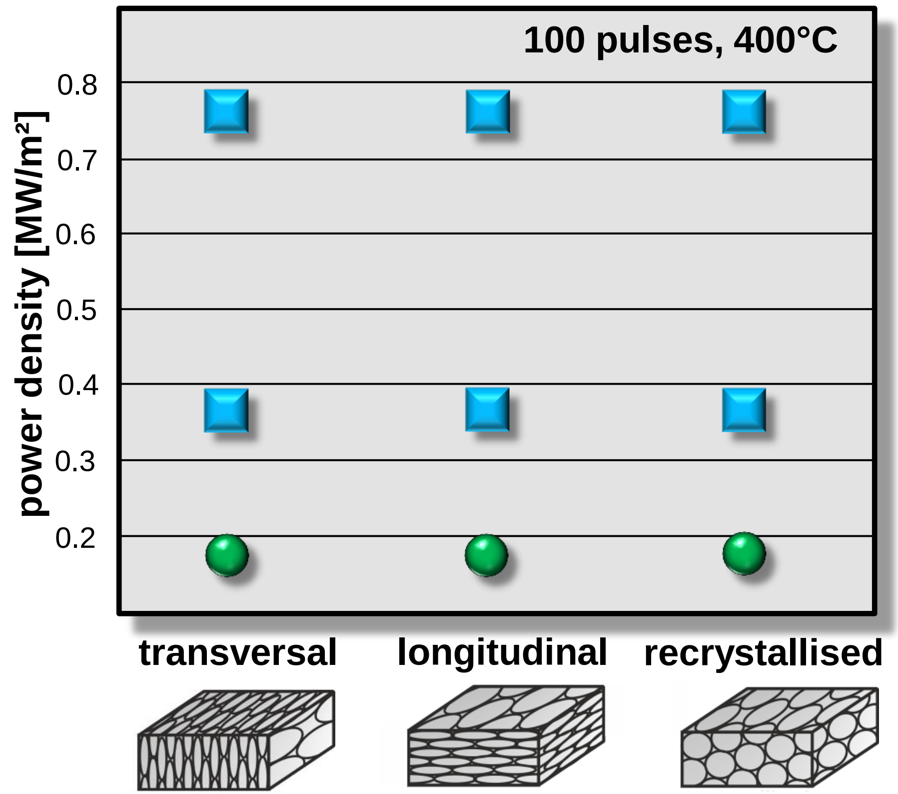

hydrogen embrittlement

- no damage
- surface modification
- cracks

Thermal shock and He-loading in PSI-2

Laser beam

1000 ELM-like events
absorbed power density: 0.76 GW/m²
pulse duration: 1 ms (f = 0.5 Hz)

He-Plasma

plasma flux: 2.8×10^{22} $m^{-2}s^{-1}$
plasma fluence: 5.6×10^{25} m^{-2}
T_{base}: 1000 – 1100 K

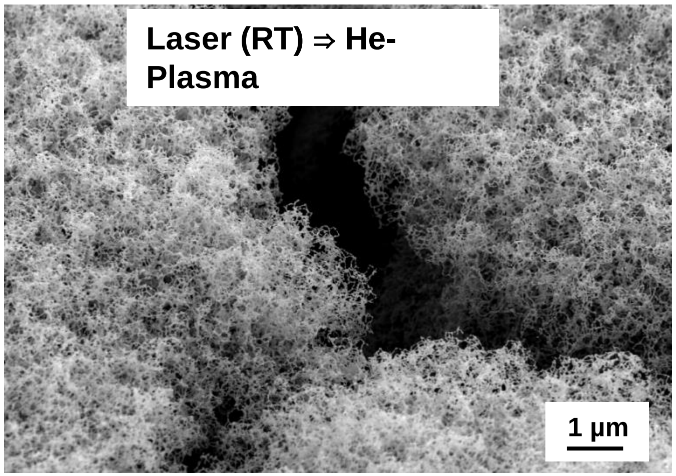

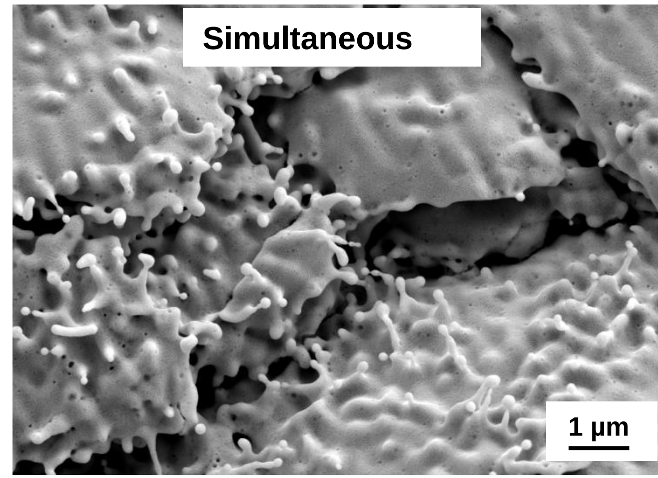

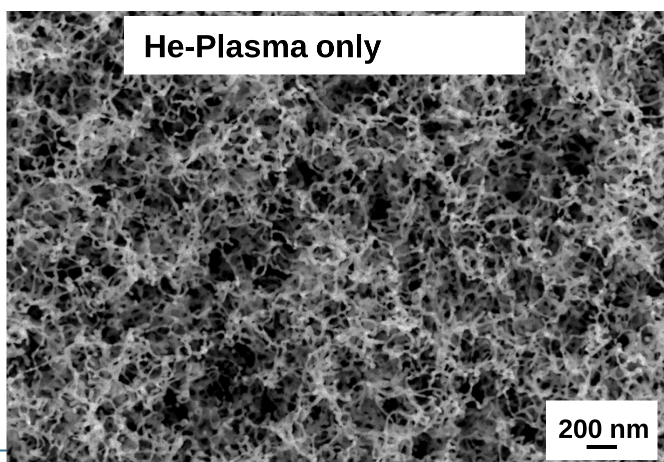

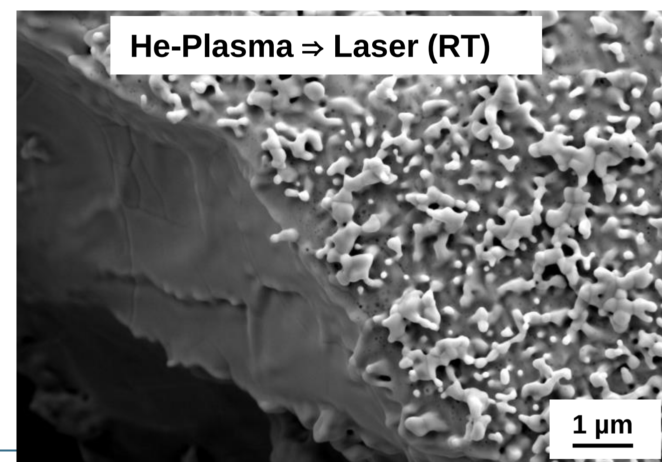

Combined tests in JUDITH 1 and GLADIS

JUDITH 1

100 pulses of 1 ms at RT

120 kV acceleration voltage

0.38 GW/m² absorbed power density

4×4 mm^2 scanned surface

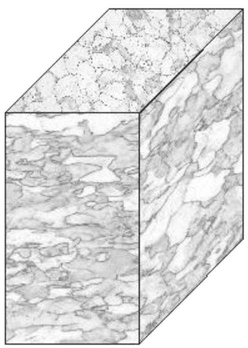

GLADIS

Beam content H or H/He$_{6\%}$

Extraction voltage 30 kV

Peak heat flux 10.5 MW m^{-2}

Peak particle flux 3.7×10^{21} m^{-2} s^{-1}

180 pulses of 30 s

Peak fluence 2×10^{25} m^{-2}

Surface 5×10 mm²
Height 5/10/15 mm
600°C/1000°C/1500°C

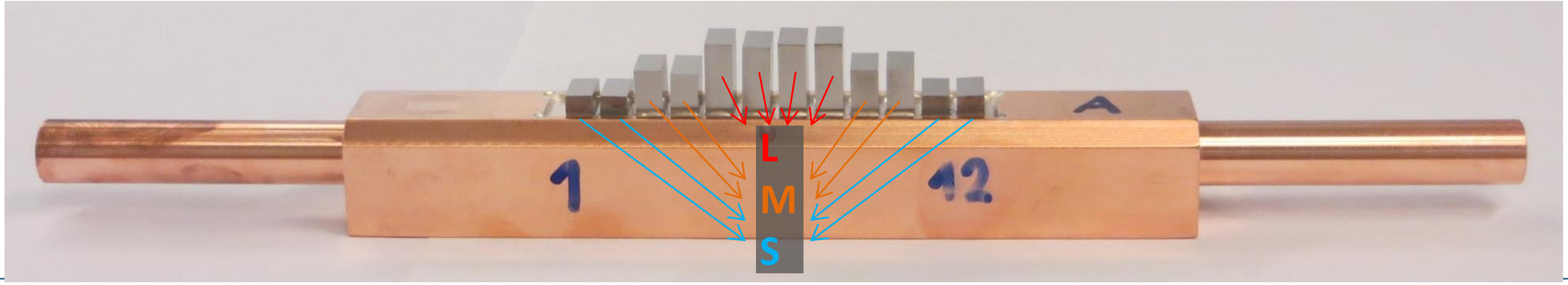

Thermal shock and H/He-loading in Gladis

Electron beam

100 ELM-like events

absorbed power density: 0.38 GW/m^2

pulse duration: 1 ms (f = 0.5 Hz)

T_{base} = 1000 °C

H/He-Plasma

plasma flux: $3.7 \times 10^{21}\ m^{-2}s^{-1}$

plasma fluence: $2 \times 10^{25}\ m^{-2}$

180 pulses of 30 s

T_{base} = 1500 °C

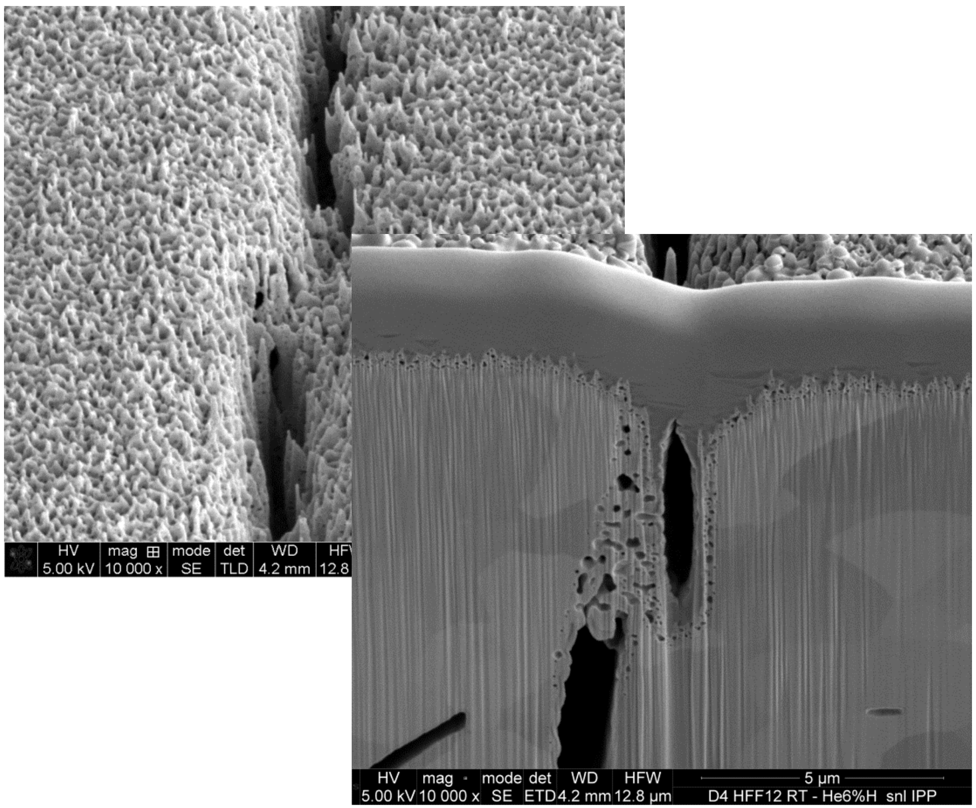

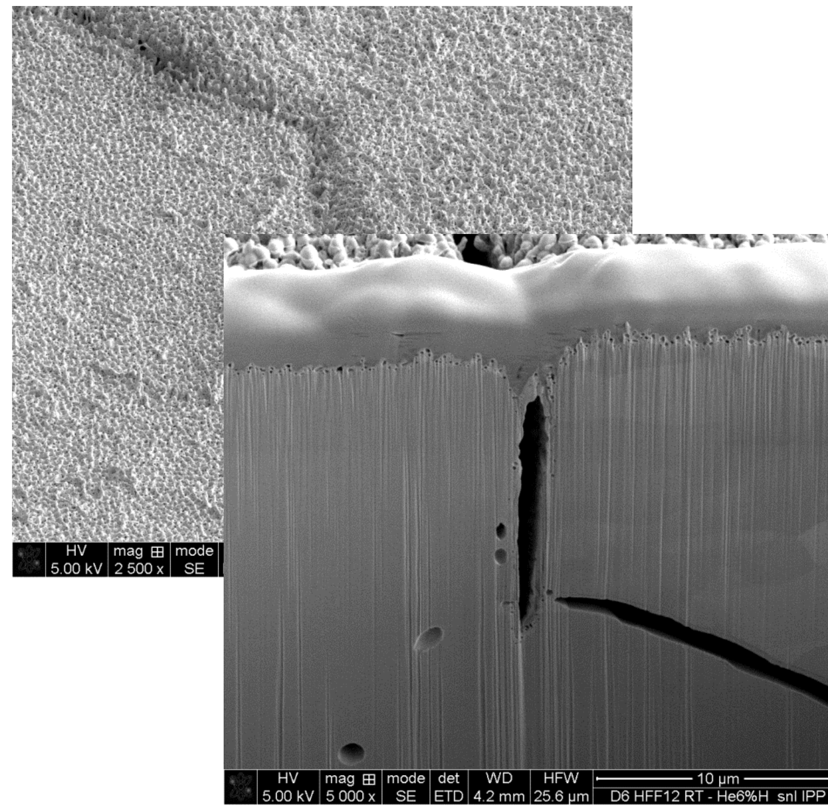

risk of erosion?

Thermal shock and H/He-loading in Gladis

H/He exposed S-sample

$T_{surface} \approx 600°C$ in GLADIS

$T_{base} \approx 1000°C$ in JUDITH 1

Base temperature effect?

Thermal shock effect?

600°C with H/He – before ELM

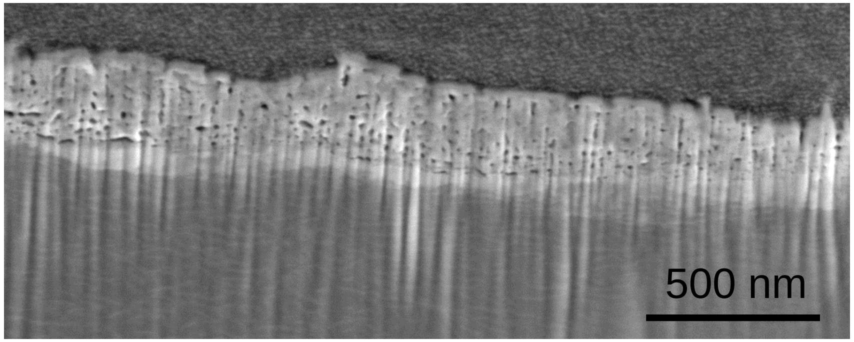

Increased gas pressure? (if cavity contains gas, despite lack of flux)

Decreased shear modulus affects the Greenwood equilibrium:

$$P_{LP} \geq 2\gamma / r_b + G\,b / r_b$$

- Surface tension γ
- Bubble radius r_b
- Shear modulus G
- Burgers vector b
- Cavity growth if pressure > P_{LP}

600°C with H/He – after ELM

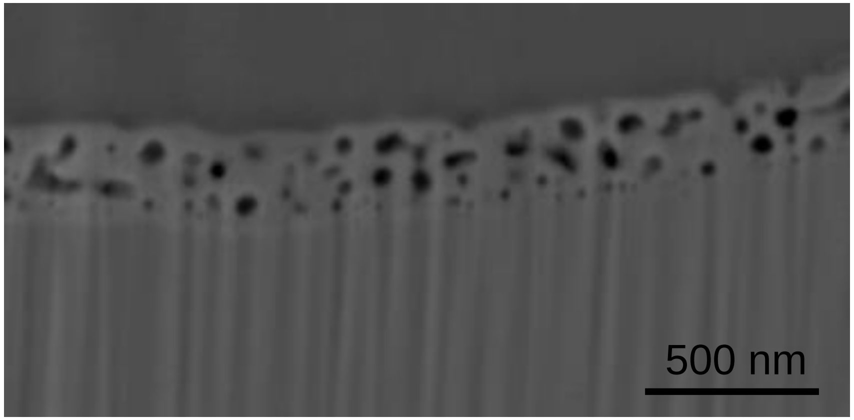

G. Greenwood et al., Journal of Nuclear Materials 1 (1959) 305-324

D

Change of W micro- structure under simultaneous heat and particle loads and impact on W erosion and fuel retention in W

Plasma exposure parameters in PSI-2

Plasma parameters

Magnetic field in exposure chamber	**0.1 T steady-state**
Plasma species	**D, H, N, Ar, He, Ne etc.**
Electron temperature	**1 - 25 eV (for D)**
El. density	**~10^{16} - 10^{19} m^{-3}**
Particle flux	**~10^{20} - 10^{23} $m^{-2}s^{-1}$**
Particle fluence	**up to ~10^{27} m^{-2} per exposure**
Incident ion energy	**~10 - 300 eV (negative bias)**
Sample temperature	**RT - 2000°C**
Diameter of plasma column	**≈ 6 cm**

Langmuir probe measurements for deuterium plasma

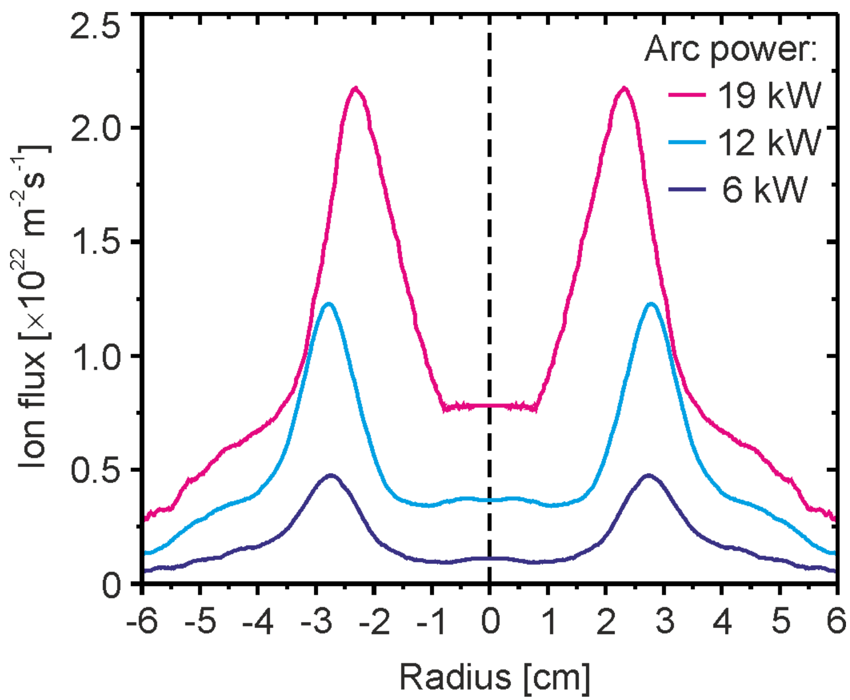

- **Transients (ELMs, disruptions) can be simulated by laser irradiation**
- **Exposure parameters can be pre-selected to simulate particular ITER conditions**

- **Hollow plasma profile due to cathode – anode geometry**
- **Sample is usually placed in region with maximum flux (r = 2.0 - 3.5 cm)**

M. Reinhart, A. Kreter, B. Unterberg, D. Matveev, M. Rasinski

Plasma exposure parameters for studies on impact of impurities on fuel retention

Incident ion flux	**~ 10^{22} $m^{-2}s^{-1}$**
Incident ion fluence	**~ 10^{26} m^{-2}**
Incident ion energy	**≈ 40 eV**
Sample temperature	**380 K**
Fraction of seeded Helium and Argon ions	**0 – 8%, controlled by spectroscopy**

Sample surface mechanically polished, annealed at 1000°C for 2 h

Deuterium retention in tungsten under influence of helium and argon

Thermal desorption spectra (TDS) of tungsten exposed to mixed plasmas

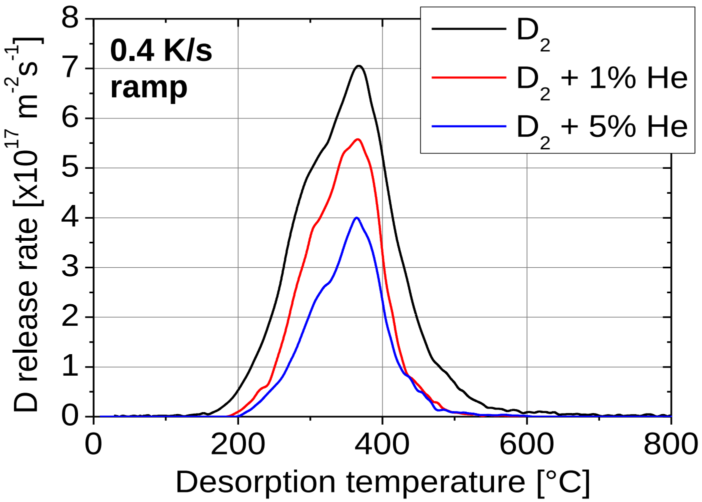

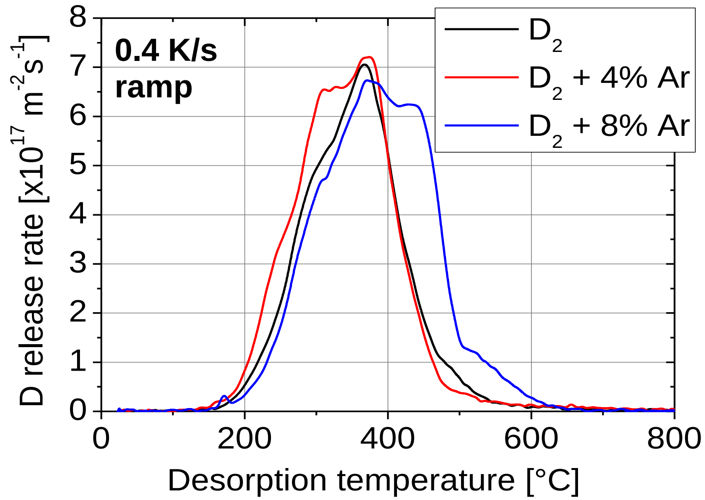

Total amount of deuterium retained in exposed tungsten

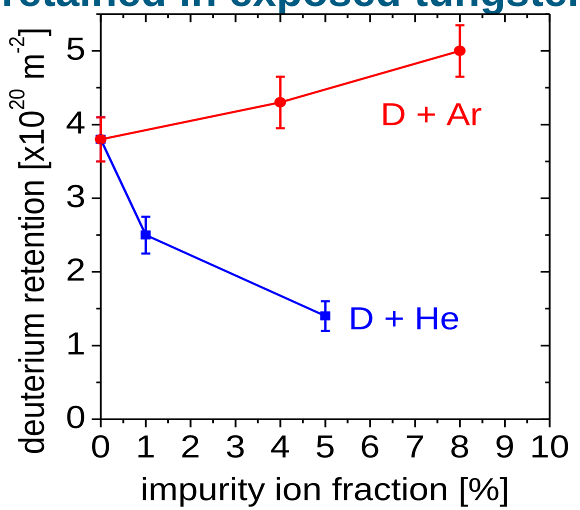

Effect of helium:

- Total deuterium retention is reduced by a factor of 3

Effect of argon:

- Total deuterium retention slightly increased
- TDS spectra show different shapes
  → Change in trapping sites due to material damage by argon

[M. Reinhart et al., J. Nucl. Mater. 463 (2015) 1021]

TEM cross-section images for D, D+He and D+Ar exposure

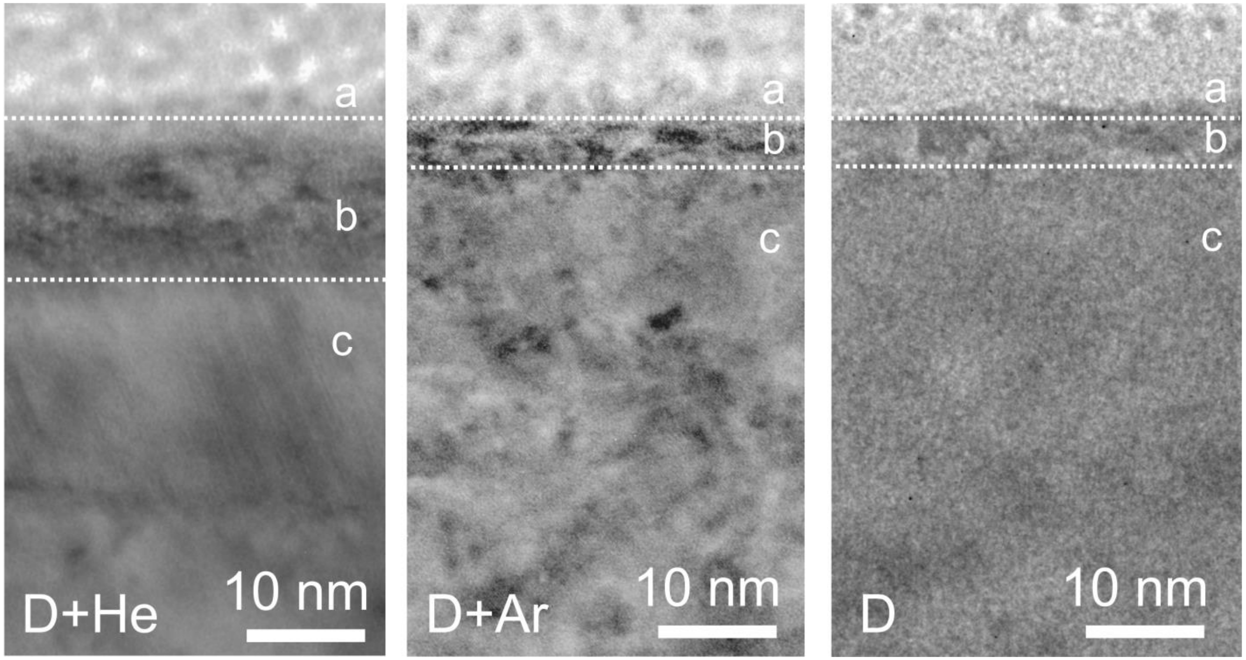

a) platinum coating

b) damaged surface layer/ He nano-bubbles

c) bulk tungsten

D, D+Ar exposures:
damaged layer depth is in the ion penetration range (2 nm)

D+He exposure:
damaged layer depth is beyond the ion penetration range
→ formation and growth of helium nano-bubble layer

Deuterium retention in tungsten for variation of incident fluences

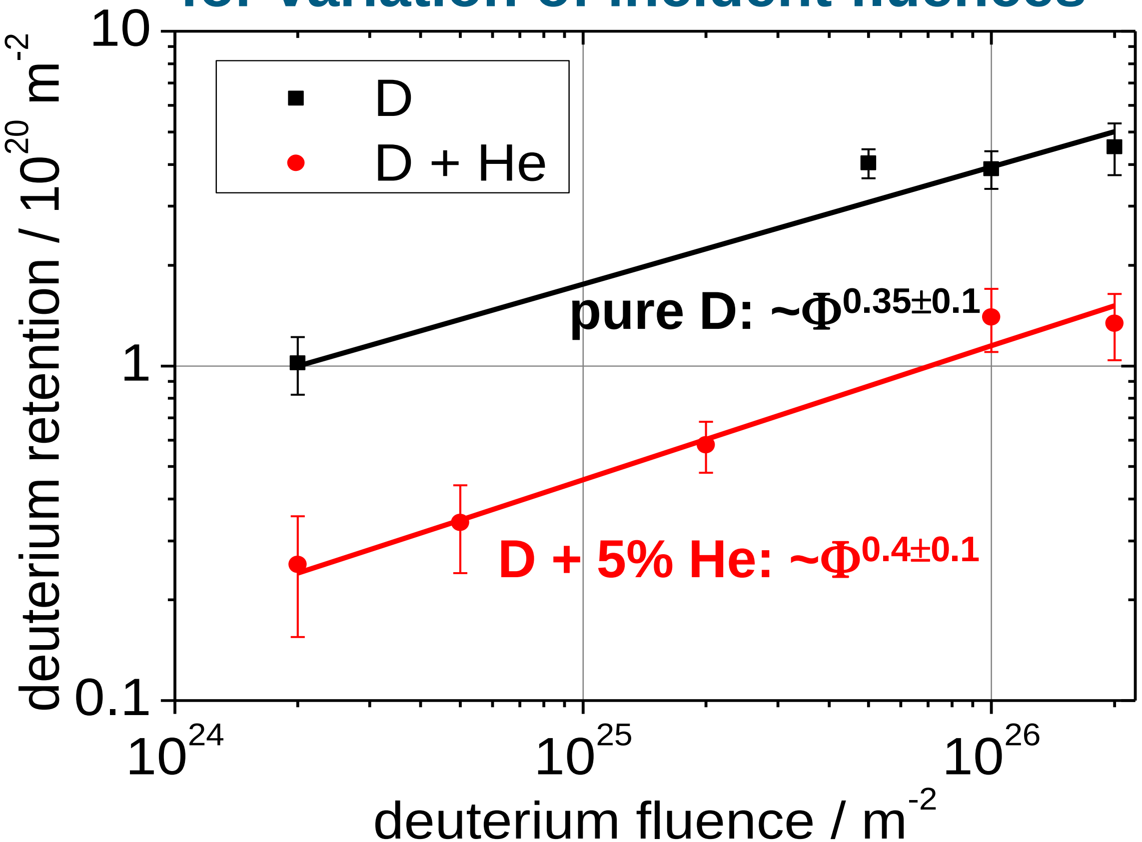

Influence of He develops at low fluences (He⁺ fluence <10^{23} m^{-2})

Reduction in retention of factor of 3-4 remains constant for the range of fluences

Blister formation in tungsten by deuterium irradiation at high surface temperatures

SEM images of tungsten exposed to

<u>low flux</u> in PSI-2 | **<u>high flux</u> in Magnum-PSI**

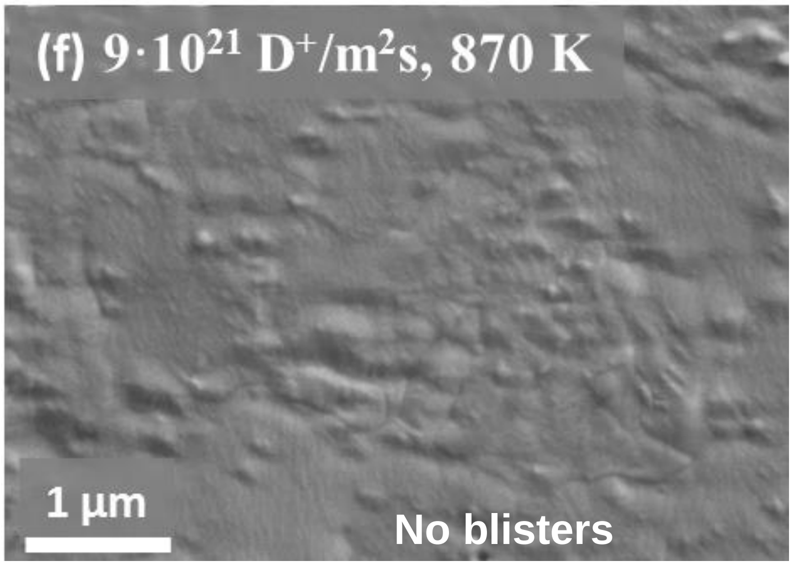

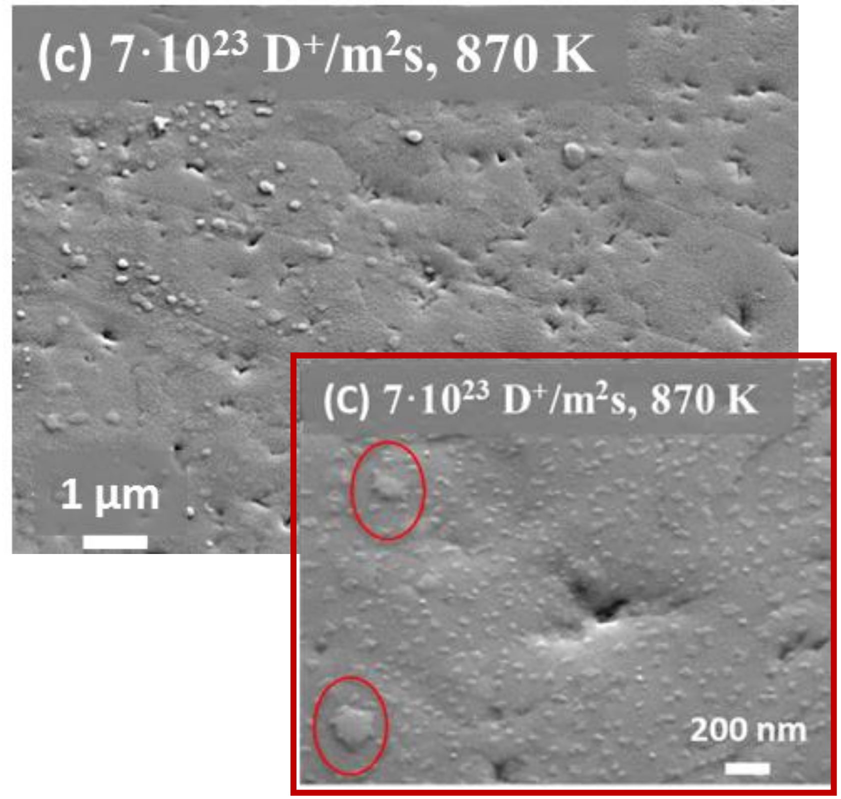

Incident ion fluence kept constant
by longer exposures in PSI-2

At high flux, blistering occurred for T_s > 800 K !

[L. Buzi et al., J. Nucl. Mater. 455 (2014) 316]

Blistering and deuterium retention in tungsten exposed to different ion fluxes

Domain of blister formation

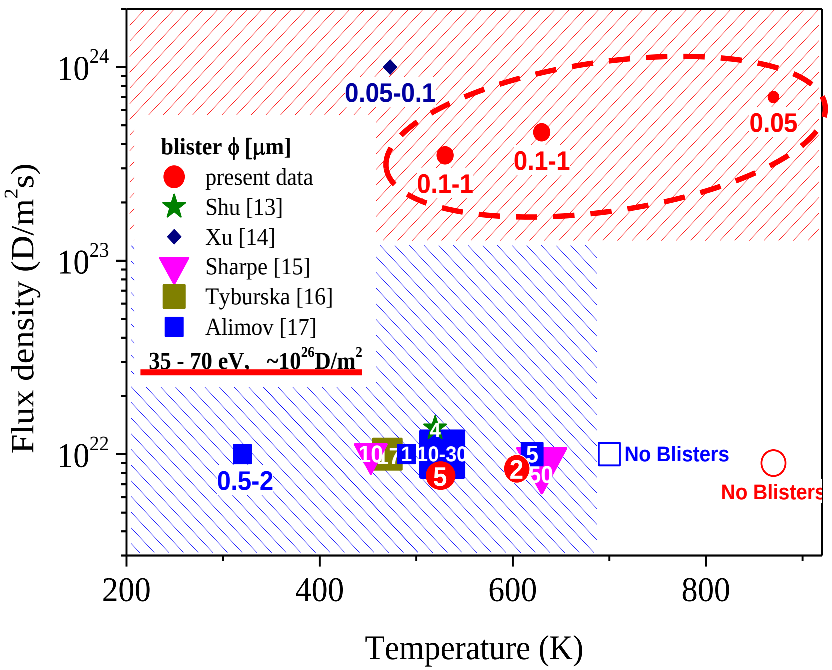

Total retention (TDS)

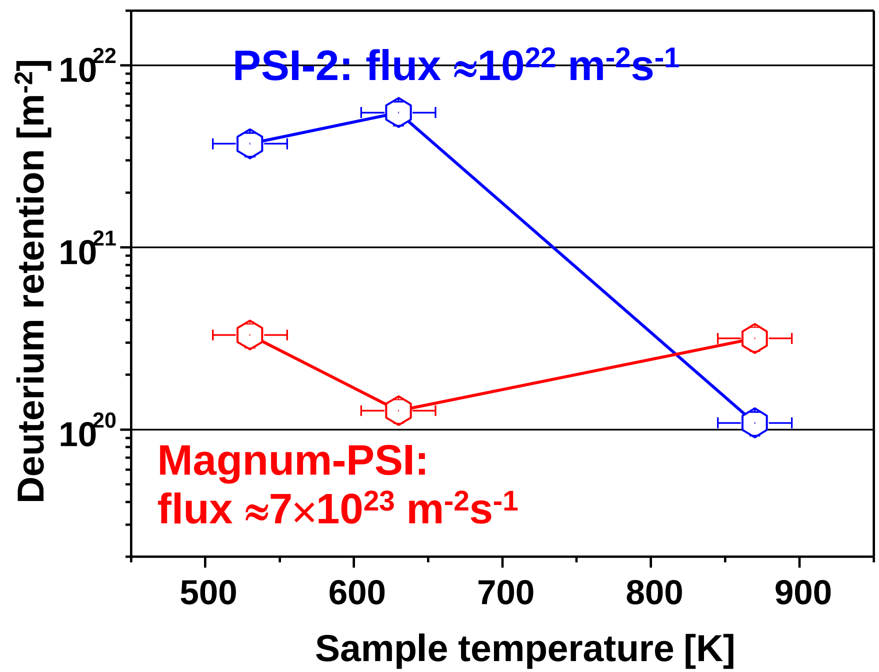

The presence of blisters correlates with the total amount of retained deuterium

At low and moderate exposure temperatures: higher retention for lower flux

At high exposure temperatures: higher retention for higher flux

[L. Buzi et al., J. Nucl. Mater. 455 (2014) 316]

E

Development of advanced tungsten materials

W-Fibre re-inforced Tungsten

Powder metallurgical Wf/W based on Hot-Isostatic Pressing

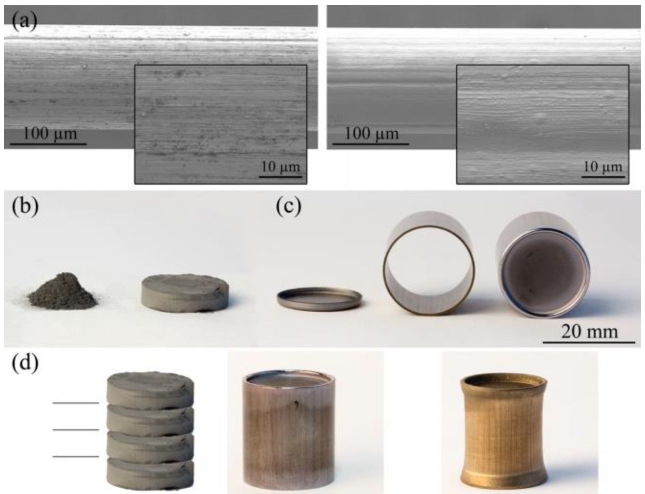

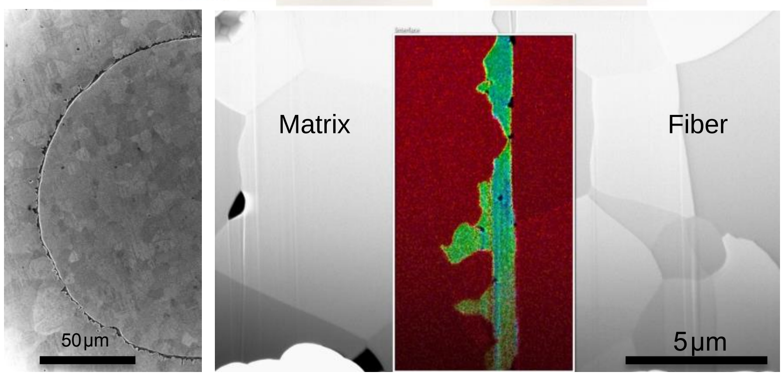

Single Fibre W_f/W , 150µm fibre , HIP Matrix
99% dens material
Er_2O_3 interface
Early development stages
Multi-fibre materials in 2016

W_f/W based on Chemical Vapor Deposition

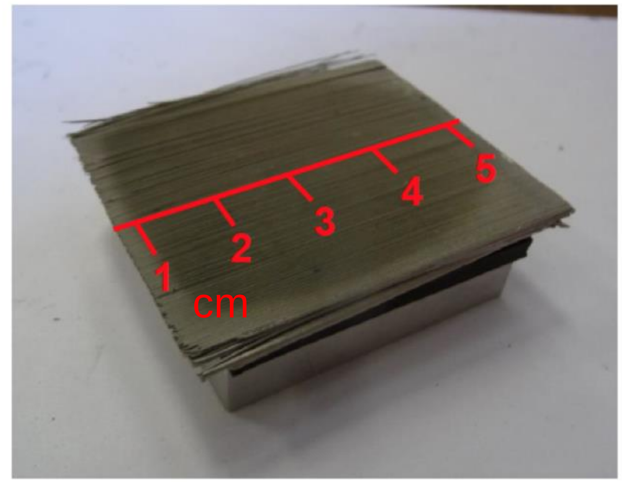

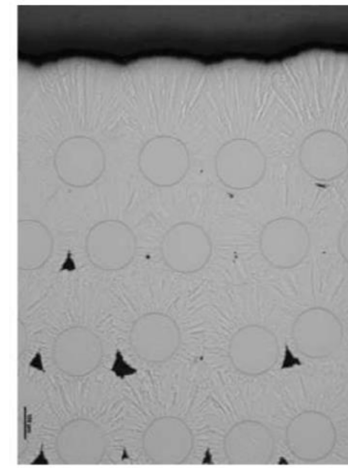

J.W. Coenen, B. Jasper, J.Riesch and T.Hoeschen

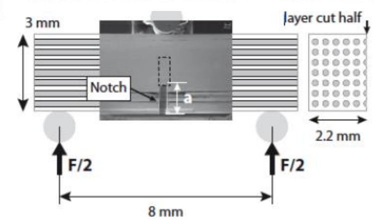

10 layers with 220 fibres (pure) each, fibre volume fraction ≈ 0.3, unidirectional
62 x 57 x 3.5-4 mm3, 194 g
94.2 % overall density
Er_2O_3 interface
Proven enhanced mechanical strength and fracture toughness
CVD Setup now available at FZJ

Smart alloys: Motivation

Conceptual study of the fusion power plant

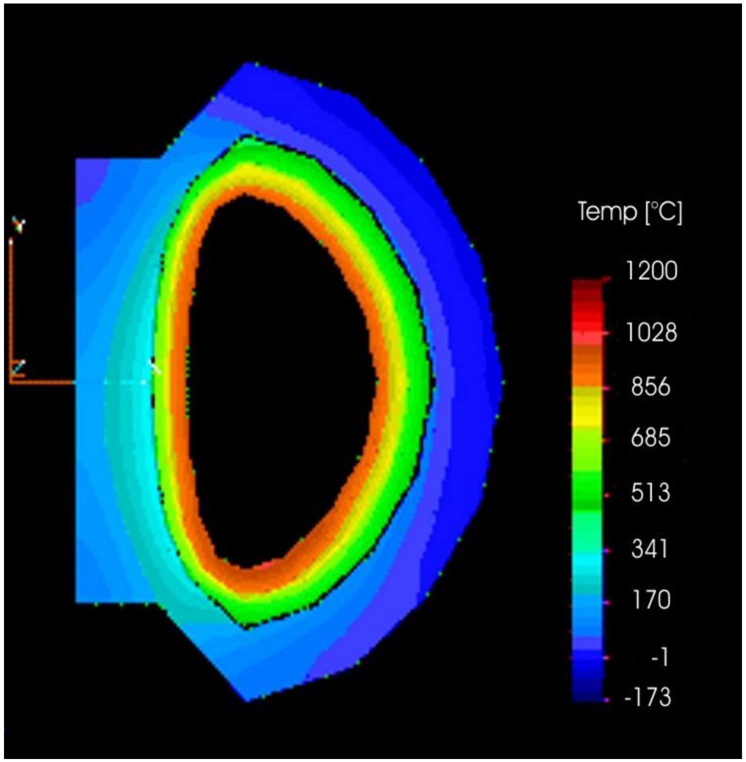

Temperature profile in PPCS Model A, 10 days after accident with a total loss of coolant.

[Final Report of the European Fusion Power Plant Conceptual Study, EFDA RP-RE 5.0, 2005]

- Accidental loss of coolant: peak temperatures of first wall up to 1200 °C due to nuclear afterheat
- Additional air ingress: formation of highly volatile WO_3 (Re, Os)
  - Evaporation rate: 10 -100 kg/h
  - >1000°C in a reactor
  - 1000 m^2 surface

Radioactive WO_3 may leave hot vessel

→ Mobilization of radioactive elements must be prevented

Tungsten-based "smart" alloys

- Behave like tungsten during plasma operation
- Suppress oxidation during accident

Ti-free alloys: oxidation tests

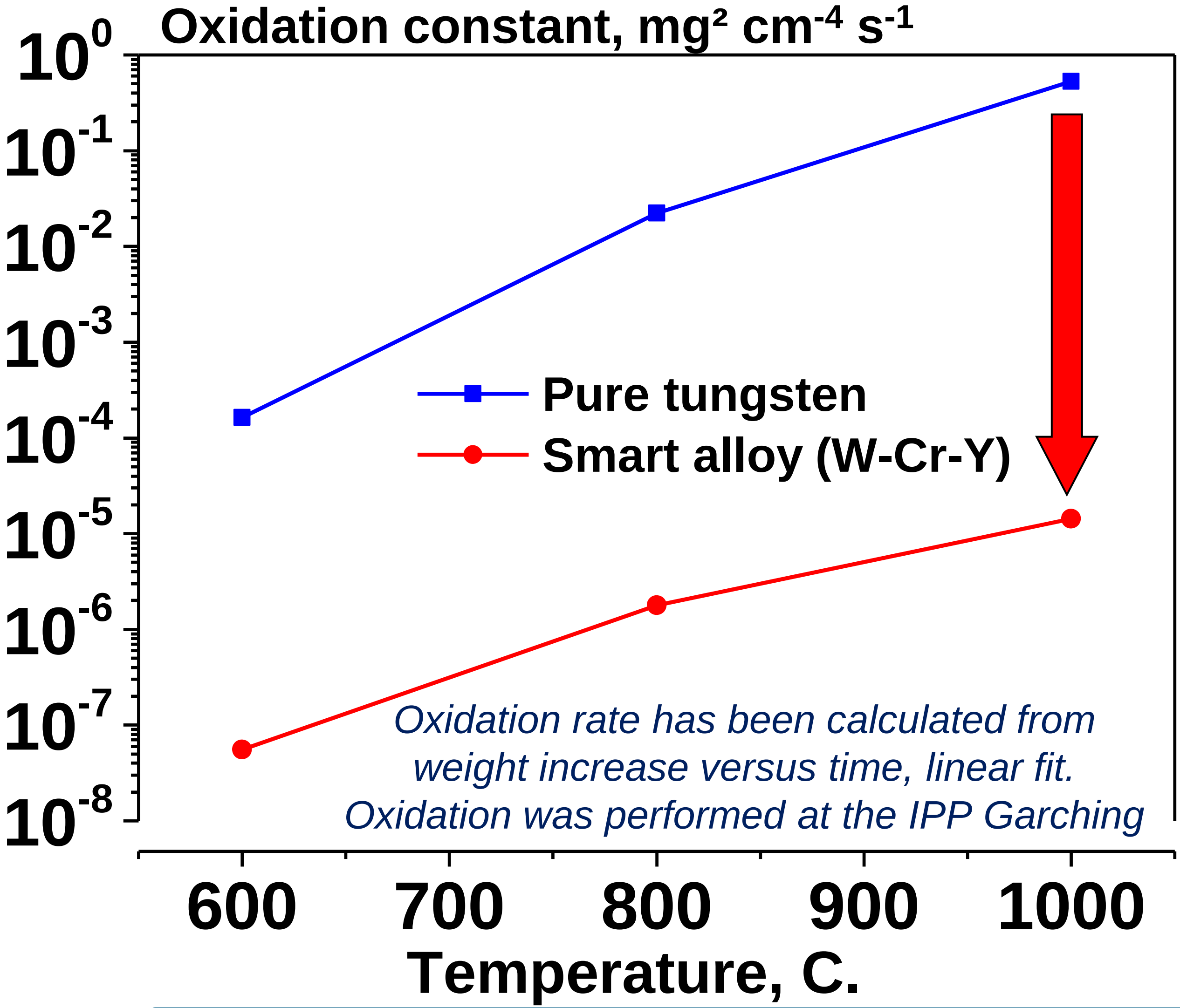

Oxidation rates (K_p) at 800ºC:

K_p (pure W) = 0.52

K_p (smart alloy W-Cr-Y) = $1.4*10^{-5}$

A. Litnovsky
T. Wegener
F. Klein

- **10^4-fold suppression of tungsten oxidation due to self passivation**
- **Tungsten fraction in the alloy is about 80 at.%**

High temperature oxidation:
W-Cr vs. W-Cr-Ti vs. W-Cr-Y alloys

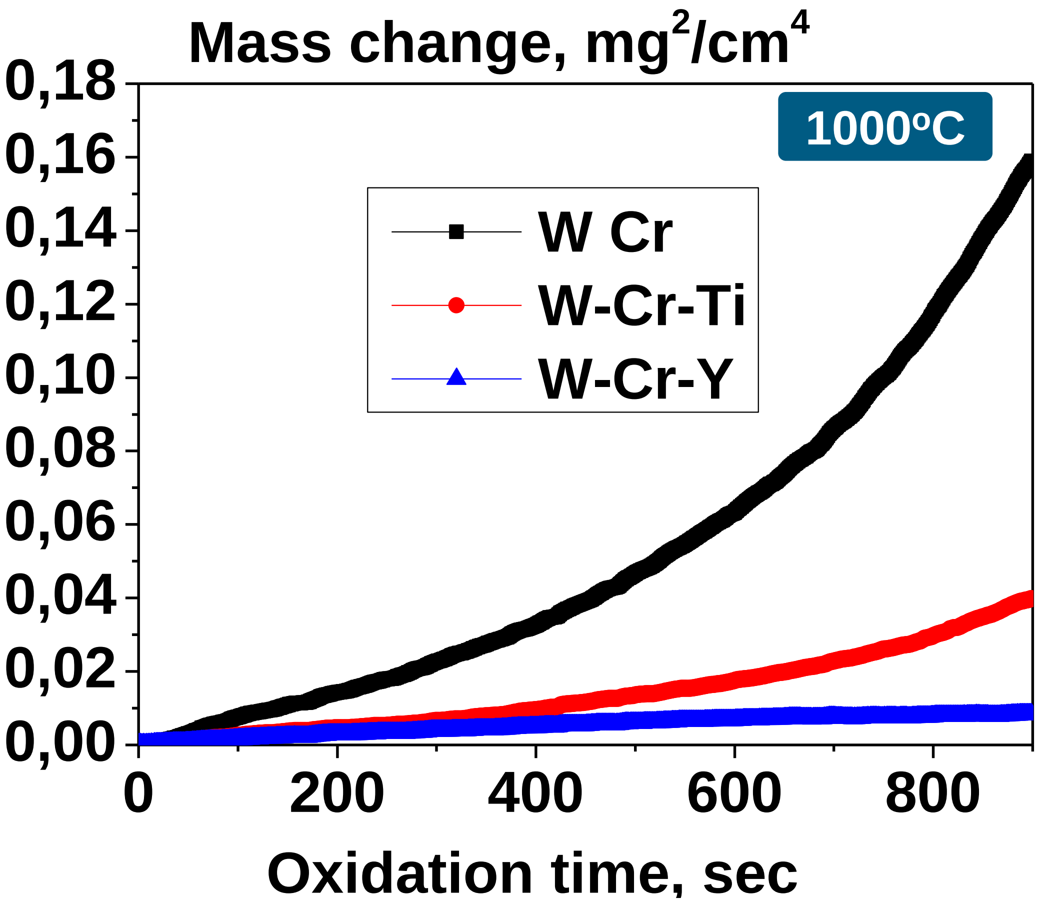

Oxidation constants

W-Cr 10.3

$K_p = 6.7 \cdot 10^{-5}\ mg^2/(cm^4 \cdot s)$

W-Cr 10.3-Ti 1.1

$K_p = 2.3 \cdot 10^{-5}\ mg^2/(cm^4 \cdot s)$

W-Cr 11.8-Y 0.3

$K_p = 6.4 \cdot 10^{-6}\ mg^2/(cm^4 \cdot s)$

→ **Best passivation behavior of W-Cr-Y alloy**

F

Tungsten characterization

W monoblock after HHF tests

SMALL SCALE MOCK-UPS

A) 1000 cycles at 10 MW/m^2

C) 1000 cycles at 10 MW/m^2 + 500 cycles at 20 MW/m^2

D) 1000 cycles at 10 MW/m^2 + 1000 cycles at 20 MW/m^2

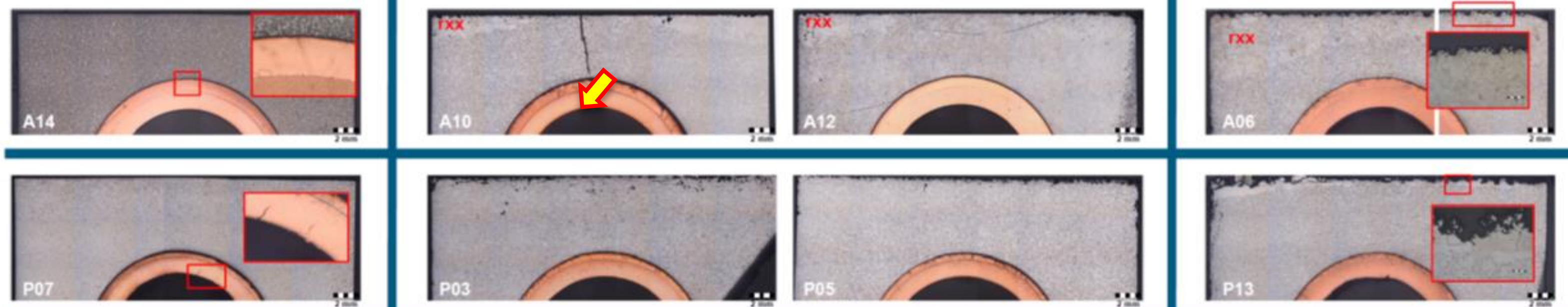

A):
- no visible defects in tungsten
- small cracks in copper

C):
- **recrystallization** → enhanced for HRP (≤ 2 mm)
- **surface roughening / erosion** → enhanced for HIP
- **cracking** → enhanced for W-sheet / HRP

D):
- **recrystallization** → HRP (2-4 mm)
- **surface roughening / melting** → peak/valley of ≤ 500 µm

VERTICAL TARGET PROTOTYPICAL COMPONENTS (VTPCs)

A) 1000 cycles at 10 MW/m^2

B) 1000 cycles at 10 MW/m^2 + 1000 cycles at 15 MW/m^2

E) 1000 cycles at 10 MW/m^2 + 1000 cycles at 15 MW/m^2 + 300 cycles at 20 MW/m^2

W Plate: 1/10 self-castellation
W bar: 8/14 self-castellation

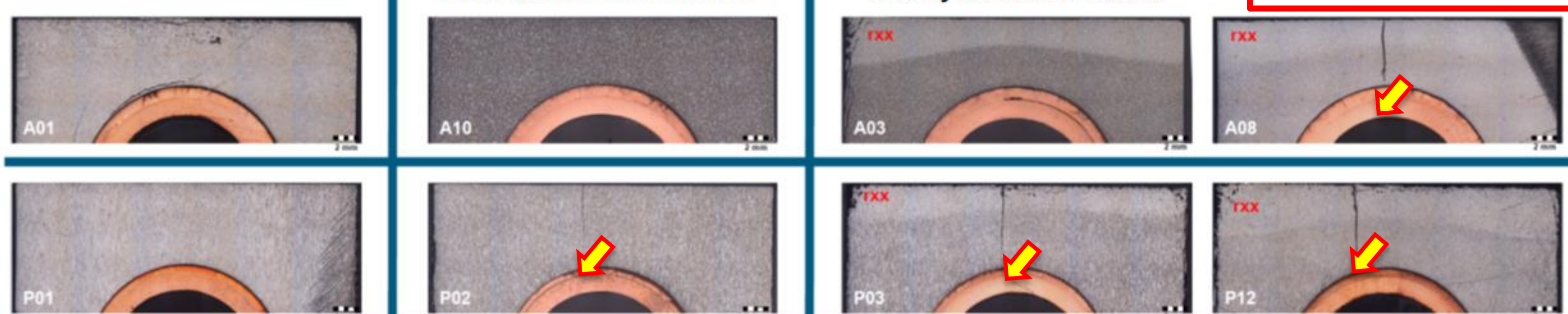

A):
- **cracking** → W-sheet / HRP® (initially existing damage?)

B):
- **cracking** → W-rod / HIP®

E):
- **recrystallization** (2-4 mm)
- **surface roughening / erosion** → enhanced for W-rod / HIP®
- **cracking**

G. Pintsuk, et al. "Qualification and post-mortem characterization of tungsten mock-ups exposed to cyclic high heat flux loading", SOFT2012 Liege BE

Difference in W materials

- Observation
  - Self-castellation often appeared in W monoblocks used by EU industry
- Conformity of W material with ITER material specification
  - Chemical composition: similar
  - Hardness: similar
  - Density: similar

	W-Plansee	W-Polema	W-ALMT	W-AT&M
HV30	441	443	461	448
density [g/cm³]	19.25	19.12	19.17	19.25

  - Microstructure: different

    N.B. production routes are different (e.g. forged bar vs rolled plates)

Forged bar

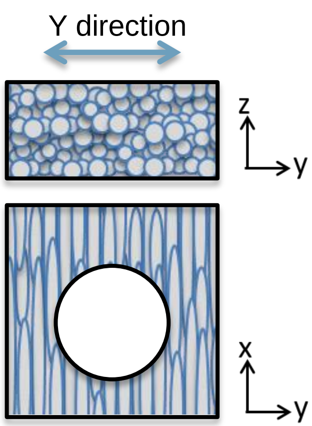

Rolled plate

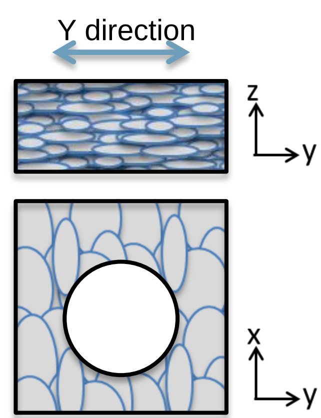

Strength in y-direction would be different

See supporting data in M. Wirtz, et al. presented at SOFT2012 http://dx.doi.org/10.1016/j.fusengdes.2013.05.07

Square sample (x- and y- direction)

Cylinder sample

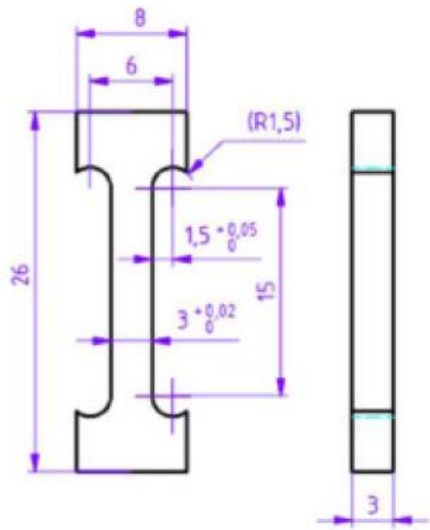

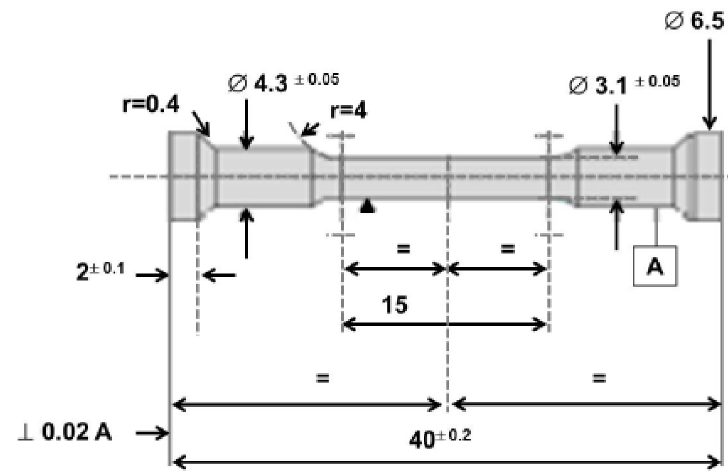

Tensile specimen

- Uniaxial Tensile Tests
  - Calibration tests on tensile specimen according to industrial standards
  - Tests on small scale samples in two directions (microstructure)
  - Strain-controlled (0.2 mm/min or 10^{-4} s^{-1})
  - Tests at elevated temperature of 800 °C
  - Tests on as-received and recrystallized samples

G

Tungsten grade for CRP
(rod material provided by Plansee)

Tungsten grade for CRP
(rod material provided by Plansee)

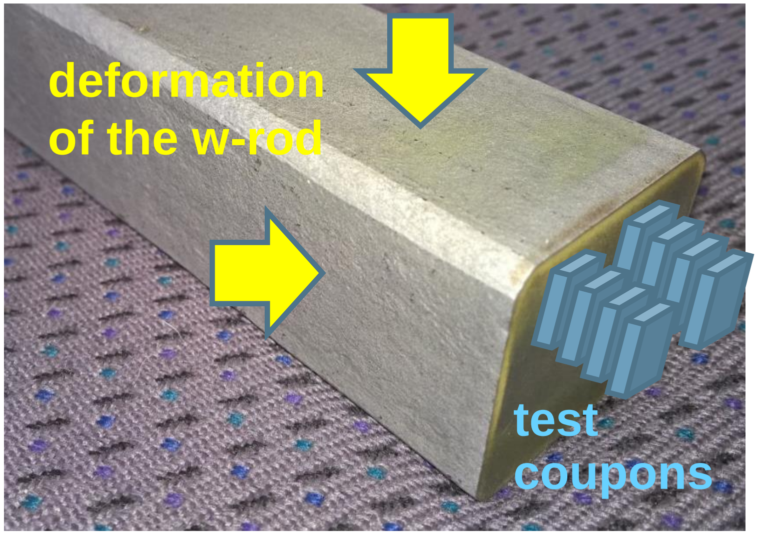

S No	Element	Manufacturer's Specifications [µg/g]	As determined by ZEA - 3 [µg/g]	Upper impurity limit	Atomic Mass
1	Al	15	< 3	3	27
2	Fe	30	7,1	7,1	55
3	Si	20			28
4	H	5	0,0001	0,0001	1
5	Cd	5	0,01	0,01	112,4
6	Cr	20	3,18	3,18	52
7	K	10	< 30	30	39,1
8	Mo	100	6	6	96
9	N	5	0,0004	0,0004	14
10	Hg	1	< 2	2	200,6
11	Cu	10	< 0.7	0,7	63,55
12	Ni	20	< 10	10	58,7
13	C	30	0,0012	0,0012	12
14	O	20	0,0004	0,0004	16
15	Pb	5	< 0,008	0,008	207,2
16	Re	0	< 0,5	0,5	186,2
17	Ta	0	< 2	2	181
18	S	0	<0,0013	0,0013	32,06
Impurities	µg	296	16,2921	64,5001	
Impurities	weight%	0,02960%	0,00163%	0,00645%	
Purity	weight%	99,970%	99,998%	99,994%	
Purity	atom%	99,76%		**99,98%**	

Summary

- Thermal shock behavior of irradiated and un-irradiated W grades
  - Synergistic effects of particle and transient heat loads on thermal shock performance of W grades
- Change of W micro- structure under simultaneous heat and particle loads and impact on W erosion and fuel retention in W
  - Fuel retention in pre-damaged W: impact of impurities (He, N, Ne, Ar) on fuel retention
  - Modification of W surface morphology under high flux/ high fluency bombardment by H and He ions and subsequent W erosion
  - Isotope exchange in damaged W – no results obtained in 2015
  - Impact of W surface contamination with oxygen on hydrogen retention and W erosion
- Development of advanced tungsten materials with improved micro-structure
- Characterization of commercially available tungsten grades
  (properties of W to be used in the frame of this CRP)